1

2 **N-terminally truncated helper NLR *NRG1C* antagonizes immunity mediated by its**

3 **full-length neighbors *NRG1A* and *NRG1B***

4

5 Zhongshou Wu[1,2], Lei Tian[1,2] and Xin Li[1,2*]

6

7 [1]Michael Smith Laboratories, University of British Columbia, Vancouver, BC V6T 1Z4,

8 Canada

9 [2]Department of Botany, University of British Columbia, Vancouver, BC V6T 1Z4, Canada

10

11 *For correspondence: xinli@msl.ubc.ca

12

13 Running title: N-terminally truncated helper NLR NRG1C is functional

14

Abstract

Both animals and plants utilize nucleotide-binding leucine-rich repeat immune receptors (NLRs) to perceive the presence of pathogen-derived molecules and induce immune responses. *NLR* genes are far more abundant and diverse in higher plants. Interestingly, truncated NLRs, which lack one or more of the canonical domains, are also commonly encoded in plant genomes. However, little is known about their functions, especially regarding the N-terminally truncated ones. Here, we show that *Arabidopsis thaliana* (*A. thaliana*) N-terminally truncated helper NLR gene *NRG1C* (*N REQUIREMENT GENE 1*) is highly induced upon pathogen infection and in autoimmune mutants. The immune response and cell death conferred by some TIR (Toll/interleukin-1 receptor)-type NLRs (TNLs) are compromised in the *NRG1C* overexpression lines. Detailed genetic analysis revealed that NRG1C antagonizes the immunity mediated by its full-length neighbors *NRG1A* and *NRG1B*. Biochemical tests indicate that NRG1C possibly interferes with the EDS1-SAG101 complex, which likely signals together with NRG1A/1B. Interestingly, Brassicaceae NRG1Cs are functionally exchangeable, and the *Nicotiana benthamiana* (*N. benthamiana*) N-terminally truncated helper NLR NRG2 antagonizes NRG1 in tobacco. Together, our study uncovers an unexpected negative role of N-terminally truncated helper NLRs in different plants.

Keywords: NLR, N-terminally truncated NLRs, Helper NLRs, NRG1C, TNL, NLR cluster, Plant immunity, NRG1

Introduction

Plants utilize a sophisticated innate immune system to defend against a plethora of pathogens. They depend on immune receptors to recognize non-self and initiate defense. Plasma membrane localized pattern-recognition receptors (PRRs) can perceive pathogen-associated molecular patterns (PAMPs), leading to PAMP/pattern-triggered immunity (PTI) (Couto and Zipfel, 2016). On the other hand, intracellular nucleotide-binding leucine-rich repeat immune receptors (NLRs) are responsible for warding off adapted pathogens by detecting their secreted effectors, thereby activating effector-triggered immunity (ETI) (Cui et al., 2015).

NLRs are present in both animals and plants. They are members of the STAND (signal transduction ATPases with numerous domains) family consisting of a variable N-terminal domain, a central nucleotide-binding (NB) motif and a C-terminal leucine-rich repeat (LRR) region (Bonardi et al., 2012; Jones and Dangl, 2006). Typical plant sensor NLRs (sNLRs) have either a Toll/interleukin-1 Receptor (TIR) or a coiled-coil (CC) domain at their N-termini, and are termed TNLs (TIR-NB-LRR) or CNLs (CC-NB-LRR), respectively (Jones et al., 2016). They have evolved to recognize effectors directly or indirectly (Baggs et al., 2017). In contrast, a small subclass of NLRs is genetically required for diverse sNLRs' immune signaling. These NLRs are termed helper NLRs (hNLR) (Bonardi et al., 2011; Collier et al., 2011; Jubic et al., 2019; Peart et al., 2005). There are two *hNLR* gene families in *A. thaliana*, encoding RNLs (RPW8 (Resistance to Powdery Mildew 8) CC-NB-LRR): the *ACTIVATED DISEASE RESISTANCE 1* (*ADR1*) family (Bonardi et al., 2011) and the *N REQUIREMENGT GENE 1* (*NRG1*) family (Peart

61 et al., 2005). Besides RNLs, the Solanaceae-specific CNL NRC (NB-LRR protein
62 required for HR-associated cell death) proteins also function as hNLRs since both cell
63 surface PRRs (Rathjen and Dodds, 2017; Wu et al., 2016) and many sNLRs signal
64 through NRCs (Gabriëls et al., 2006; Gabriëls et al., 2007; Wu et al., 2017a). In
65 comparison to the highly divergent sensor TNLs and CNLs, hNLRs are evolutionarily
66 more conserved (Adachi et al., 2019; Andolfo et al., 2019; Shao et al., 2016; Wu et al.,
67 2017a; Zhong and Cheng, 2016).
68
69 Plant *sNLRs* are among the most rapidly evolving genes (Gao et al., 2018; Guo et al.,
70 2011; Van de Weyer et al., 2019). As a result, they are highly polymorphic. *NLR* allelic
71 diversity mainly depends on the generation of either chimeric LRRs by intra- and
72 intergenic recombination and gene conversion (Serra et al., 2018), or novel LRRs through
73 point mutations (Lu et al., 2016; Mago et al., 2015; Michelmore and Meyers, 1998;
74 Tamborski and Krasileva, 2020). Gene clustering is another feature commonly observed
75 for plant *NLRs* (Van de Weyer et al., 2019). Two types of cluster patterns exist based on
76 the diversity of *NLRs* within (Jacob et al., 2013). Homogenous clusters contain the same
77 type of *NLRs* derived from tandem duplications. In contrast, heterogeneous clusters
78 contain diverse *NLRs* generated by ectopic or large-scale segmental duplications (Jacob
79 et al., 2013; Krasileva, 2019; Marone et al., 2013). Pan-genome analysis reveals that *NLR*
80 cluster patterns vary among *A. thaliana* accessions. Some clusters have highly conserved
81 copy numbers, while others show huge variations (Lee and Chae, 2020). An increasing
82 number of examples suggest that clustered NLRs often are co-expressed and may
83 cooperate to function. Clustering *sNLRs* together has the potential to massively expand

84 pathogen recognition by increasing their oligomerization options (van Wersch and Li,
85 2019).
86
87 Duplication and uneven crossover events may generate *NLRs* lacking one or more of the
88 canonical domains, yielding truncated *NLRs* (Baggs et al., 2017; Wicker et al., 2007),
89 which are commonly found in all plant genomes (Bai et al., 2002; Jacob et al., 2013; Lee
90 and Chae, 2020; Meyers et al., 2003; Meyers et al., 2002; Van de Weyer et al., 2019;
91 Yang et al., 2008). Interesting, most truncated NLRs are expressed (Meyers et al., 2002;
92 Nandety et al., 2013; Tan et al., 2007), suggesting their potential role in plant immunity.
93 Several C-terminally truncated NLRs have been studied. For instance, *A. thaliana* TIR-
94 only protein RBA1 (RESPONSE TO HOPBA1) is specifically required for defense
95 responses mediated by bacterial effector HopBA1 (Nishimura et al., 2017). Another well-
96 studied example includes the *A. thaliana* TN (TIR-NB) proteins CHS1 (CHILLING
97 SENSITIVE 1) and TN2. CHS1 and TN2 form distinct pairs with full-length TNL SOC3
98 (SUPPRESSOR of *chs1-2*, 3) to monitor the homeostasis of E3 ligase SAUL1
99 (SENESCENCE-ASSOCIATED E3 UBIQUITIN LIAGASE 1) (Liang et al., 2019; Tong
100 et al., 2017). However, little is known about the functions of N-terminally truncated
101 NLRs, including NL (NB-LRR) and LRR proteins.
102
103 Although hNLRs may not have effector recognition capabilities, the NRG1-type *hNLRs*
104 are organized in clusters in various plant species (Andolfo et al., 2019; Jubic et al., 2019;
105 van Wersch and Li, 2019; Wu et al., 2019). In contrast, *ADR1s* are scattered in the
106 genome (Bonardi et al., 2011; Dong et al., 2016). There are three *NRG1* paralogs in the *A.*

107 *thaliana* genome: full length *NRG1A* and *NRG1B,* and N-terminally truncated *NRG1C*
108 (Jubic et al., 2019; Wu et al., 2019). *NRG1A* and *NRG1B* are present in the *NRG1* cluster
109 across almost all analyzed *A. thaliana* and *A. lyrate* accessions (Lee and Chae, 2020).
110 *NRC1C* encodes a predicted protein missing the RPW8 CC domain and most of the NB
111 domain. Similarly, *N. benthamiana* contains a copy of the full-length *NRG1* and an N-
112 terminally truncated *NRG2*. In comparison to the clustered *NRG1s* in *A. thaliana*, *NRG2*
113 does not cluster with *NRG1* and has been assumed to be a pseudogene (Peart et al., 2005).
114 It is unclear whether these N-terminally truncated hNLRs have any biological roles.
115
116 Here, we describe the functional analysis of truncated hNLRs. To our surprise, NRG1C
117 negatively regulates TNL autoimmune mutant *chs3-2D* (*chilling sensitive 3, 2D*)-
118 mediated autoimmunity, serving an opposite role from its full-length paralogs
119 NRG1A/1B. *NRG1C* overexpression plants phenocopy those of the *nrg1a nrg1b* double
120 mutant or the *sag101* (*SENESCENCE-ASSOCIATED GENE 101*) single mutant.
121 Biochemical analysis indicates that NRG1C possibly works by interfering with the EDS1
122 (ENHANCED DISEASE SUSCEPTIBILITY 1)-SAG101 complex. Interestingly,
123 Brassicaceae NRG1Cs from different species are functionally exchangeable. In addition,
124 the *N. benthamiana* truncated NRG2 also antagonizes NRG1-mediated cell death. In
125 summary, our study uncovers an unexpected role of N-terminally truncated hNLRs,
126 which was likely evolved to balance the activities of their corresponding full-length
127 hNLRs.
128
129

130 **Results**

131

132 ***NRG1C* is evolutionarily conserved in Brassicaceae and its expression is highly**
133 **induced in TNL-type autoimmune mutants and upon pathogen infection**

134

135 BLASTp analysis revealed that NRG1C (AT5G66890)-type N-terminally truncated
136 hNLRs are present in all 8 well-sequenced Brassicaceae species and *N. benthamiana*
137 (Figure 1A-B and Figure S1). Additionally, *NRG1C* is present in most *A. thaliana*
138 accessions. However, no NRG1C ortholog was found in available protein databases of
139 other land plants. Interestingly, as with *A. thaliana NRG1C*, other Brassicaceae *NRG1C*
140 orthologs also tend to cluster with the full length *NRG1* genes in their genomes (Table
141 S1). Phylogenetic analysis indicates that all Brassicaceae NRG1Cs came from the same
142 ancestor (Figure 1B). The Brassicaceae *NRG1C* genes likely originated from either an
143 initial gene duplication from the *NRG1A/1B* ancestor and a subsequent N-terminal loss,
144 or partial gene duplication. In contrast, NbNRG2 and NbNRG1 belong to a distinct clade
145 from Brassicaceae NRG1, suggestive of an independent evolution of NbNRG1 (Figure
146 1B and Figure S1). In *Brassica rapa*, there are two close NRG1C homologs found in two
147 separate gene clusters. Brara.I00877.1 and Brara.G01211.1 share 75.4% and 62.0%
148 amino acid identity, or 86.2% and 75.5% similarity with NRG1C, respectively (Figure
149 S1). However, phylogenetic analysis indicates that Brara.G01211.1 might not be an
150 NRG1C ortholog as it contains a full-length NB domain (Figure S1) and is evolutionarily
151 separate from the NRG1C clade (Figure 1B).

152

153 DAR5 (AT5G66630, DA1-RELATED PROTEIN 5) was proposed to be a chimeric
154 protein resulting from a translocation of NRG1C and a fusion with a member of the

155 nearby cluster carrying DAR homologs, DAR7 (AT5G66610) to DAR3 (AT5G66640)
156 (Meyers et al., 2003). Coincidently, DAR5 carries RPW8, NB and LIM (Lin11, Isl-1 &
157 Mec-3) domains, but no LRRs. It shares high similarity with NRG1s in *A. thaliana*
158 (Andolfo et al., 2019; Castel et al., 2019). However, DAR5 seems to be unique in *A.*
159 *thaliana*, as BLAST searches failed to identify putative DAR5 orthologs in genomes of
160 all other sequenced plant species.

161

162 To test whether the truncated *NRG1C* and *DAR5* are involved in TNL-mediated
163 immunity, their expression levels were first measured in TNL autoimmune mutants. *snc1*
164 (*suppressor of npr1-1, constitutive 1*) and *chs3-2D* contain gain-of-function mutations in
165 the *TNLs SNC1* and *CHS3*, respectively, resulting in TNL-mediated autoimmunity.
166 *NRG1C* transcripts were around 200 and 7000-fold up-regulated respectively in *snc1* and
167 *chs3-2D* mutants as compared with that of Col-0 wild-type (WT) (Figure 1C). However,
168 no significant *DAR5* transcript changes were observed (Figure 1D). Furthermore, the
169 transcript of *NRG1C*, but not *DAR5*, was highly induced in WT plants upon infection by
170 virulent bacterial pathogen *Pseudomonas syringae* pv. *maculicola* (*P.s.m.*) ES4326
171 (Figure 1E). These expression analyses suggest that *NRG1C* in the *NRG1* gene cluster
172 may play roles in plant biotic responses against pathogens.

173

174 ***NRG1C*, but not *DAR5*, negatively regulates *chs3-2D* and *snc1*-mediated**
175 **autoimmunity**

176

177 As *NRG1C* is up-regulated in autoimmune mutants and during infection, and the *nrg1c*
178 knockout does not seem to exhibit severe immune related defects and affect *snc1*

179 autoimmunity (Wu et al., 2019), we used an overexpression approach to examine the role
180 of these truncated NLRs. *NRG1C* and *DAR5* were individually overexpressed in *chs3-2D*
181 and *snc1* backgrounds. To our surprise, overexpression of *NRG1C* fully suppressed *chs3-*
182 *2D*-mediated dwarfism (Figure 2A-C) and enhanced disease resistance to the oomycete
183 pathogen *Hyaloperonospora arabidopsidis* (*H.a.*) Noco2 (Figure 2D). In contrast, no
184 suppression of *chs3-2D*-mediated growth defects was observed upon *DAR5*
185 overexpression (Figure S2A-B). Furthermore, overexpressing *NRG1C* (Figure 2E) could
186 partially suppress *snc1*-mediated dwarfism to a similar level as the *NRG1* deletion mutant
187 (Wu et al., 2019) (Figure 2F-G). Consistently, enhanced disease resistance to *H.a.* Noco2
188 (Figure 2H) and *P.s.t.* DC3000 (Figure 2I) in *snc1* were partially suppressed upon
189 *NRG1C* overexpression. However, the *snc1 DAR5 OE* lines did not show significant
190 differences in growth compared with *snc1* (Figure S2C-D). Taken together, NRG1C
191 negatively regulates *chs3-2D* and *snc1*-mediated autoimmunity with different strengths.
192 Intriguingly, these phenotypes closely resemble those of the *nrg1a nrg1b* double mutant
193 and the *sag101* single mutant (Wu et al., 2019; Xu et al., 2015).
194

195 **ADR1-L3 is dispensable for *snc1*-mediated autoimmunity and RPP4-mediated**
196 **immunity**
197

198 Similar to NRG1C in the NRG1 family, the *A. thaliana* ADR1 helper NLR family
199 includes a truncated ADR1-L3, missing the N-terminal RPW8 domain (Figure S3). In
200 contrast to the broad presence of NRG1C in Brassicaceae, an ADR1-L3 ortholog is only
201 found in *Boechera stricta* (Figure S3). To test whether ADR1-L3 is involved in immunity
202 conferred by ADR1-dependent NLRs, *ADR1-L3* was overexpressed in *snc1* background.

203 As shown in Figure S4A-B, *snc1*-mediated growth defects (Figure S4A) and enhanced
204 disease resistance (Figure S4B) were not altered upon *ADR1-L3* overexpression.
205 Furthermore, *ADR1-L3* overexpression lines in WT were not susceptible to oomycete
206 pathogen *H.a.* Emwa1 (Figure S4C), which is recognized by ADR1-dependent TNL
207 RPP4 (*RECOGNITION OF PERONOSPORA PARASITICA 4*) (Bonardi et al., 2011;
208 Dong et al., 2016). Taken together, unlike NRG1C, ADR1-L3 does not seem to play any
209 roles in TNL-mediated autoimmunity and defense.
210
211 **Overexpression of *NRG1C* has no effect on *chs1-2*- and *chs2-1*-mediated**
212 **autoimmunity, RPS2 and RPS4-mediated immunity, or basal defense**
213
214 To further test the specificity of NRG1C, *NRG1C* was overexpressed in additional
215 autoimmune mutants. In *chs1-2* (*chilling sensitive 1*, *2*), a missense mutation in a
216 truncated TN protein (Wang et al., 2013) results in constitutive cell death and defense
217 responses at low temperatures (Zbierzak et al., 2013). Another chilling sensitive mutant
218 *chs2-1* contains a gain-of-function mutation in the TNL *RPP4* (Huang et al., 2010).
219 However, neither *chs1-2* nor *chs2-1*-mediated temperature-dependent autoimmunity was
220 suppressed upon *NRG1C* overexpression (Figure S5A-B). Consistently, oomycete
221 pathogen *H.a.* Emwa1 failed to grow in *NRG1C OE* lines in the WT background (Figure
222 S5C-D).
223
224 We also challenged two independent *NRG1C OE* lines (in WT Col-0 background) with
225 *P.s.t.* DC3000 expressing either AvrRps4 or AvrRpt2 effectors, which are recognized by
226 TNL RPS4 (RESISTANT TO *P. SYRINGAE* 4) or CNL RPS2 (RESISTANT TO *P.*

227 *SYRINGAE* 2), respectively. However, no altered disease resistance against these
228 avirulent pathogens was detected (Figure S6A-B). When challenged with *P.s.t.* DC3000,
229 *NRG1C OE* lines exhibited similar bacterial growth as WT, suggesting that
230 overexpression of *NRG1C* does not compromise basal defense response either (Figure
231 S6C). Therefore, NRG1C seems to be specific to TNL-mediated immune response with
232 unequal strengths for distinct TNLs. The differential contributions of NRG1C in TNL
233 signaling are reminiscent of the phenotypes of *nrg1a nrg1b* or *sag101* knockouts, which
234 play major roles in *chs3-2D* but relatively mild roles in *snc1*, but no roles in *chs1-2*, *chs2-*
235 *1*, RPS4 and RPS2-mediated autoimmunity and bacterial growth (Castel et al., 2019;
236 Feys et al., 2005; Wu et al., 2019; Xu et al., 2015).
237
238 **NRG1C is required for HopQ1-1-mediated defense**
239
240 NbNRG1 is essential for immune signaling triggered by effector HopQ1-1 (Qi et al.,
241 2018). As *P.s.t.* DC3000 carries diverse effectors that can mask the effects of HopQ1-1,
242 *P.s.t.* CUCPB5500 in which all 18 of the well-expressed T3SS (Type III secretion
243 system) effectors were deleted, was used as a background to avoid interference from
244 other effectors (Kvitko et al., 2009). When challenged with *P.s.t.* CUCPB5500, no
245 bacterial growth difference was observed between *NRG1C OE* lines, *nrg1a nrg1b* double
246 or *sag101-1* mutants as compared with WT (Figure 3A). However, WT exhibited
247 enhanced disease resistance to *P.s.t.* CUCPB5500 expressing HopQ1-1, suggesting that
248 unidentified R proteins can likely recognize HopQ1-1 in *A. thaliana*. Consistently with
249 the observation in tobacco, this bacterial growth inhibition was largely compromised in
250 *NRG1C OE* lines, *nrg1a nrg1b* double mutant and *sag101* single mutant to a similar level

251 (Figure 3A). Taken together, NRG1C antagonizes HopQ1-1-mediated defense responses
252 in *A. thaliana*. *NRG1C* overexpression phenotypes seem identical to those of the *nrg1a*
253 *nrg1b* double and the *sag101* single mutants.
254

255 **NRG1C antagonizes AvrRPS4-mediated hypersensitive response**
256

257 AvrRPS4 can activate RRS1 (RESISTANT TO RALSTONIA SOLANACEARUM
258 1)/RPS4 pairs, resulting in hypersensitive response (HR) in Col-0 background (Saucet et
259 al., 2015). This HR is compromised in Col-0 *nrg1a nrg1b* double mutant, although no
260 difference in *P.s.t.* AvrRPS4 bacterial growth can be observed (Figure S6A) (Castel et al.,
261 2019; Lapin et al., 2019). We thus tested whether NRG1C regulates RRS1/RPS4-
262 mediated HR. Effector AvrRPS4 was delivered using *P. fluorescens* strain *Pf0-1*
263 containing type III secretion system (*Pf0-1* EtHAn), but lacking type III effector genes
264 (Thomas et al., 2009). Similar with the phenotype of *nrg1a nrg1b* double mutant (Castel
265 et al., 2019; Lapin et al., 2019), RRS1/RPS4-mediated HR is lost in *NRG1C OE* lines
266 (Figure 3B-C). The striking overall phenotypic resemblance between *NRG1C OE* lines
267 and the *nrg1a nrg1b* double mutant indicates that NRG1C might function
268 antagonistically with NRG1A/1B in *A. thaliana* to regulate defense responses.
269

270 **NRG1C antagonizes the NRG1-SAG101 module, in parallel with the ADR1-PAD4**
271 **module**
272

273 The similar phenotypes of *adr1 triple* with *pad4* (Phytoalexin deficient 4) mutants (Dong
274 et al., 2016), and the additive effects between SAG101 and PAD4 (Rietz et al., 2011) or
275 NRG1s and ADR1s (Lapin et al., 2019; Saile et al., 2020; Wu et al., 2019) allude to an

276 EDS1-ADR1-PAD4 signaling module that works in parallel with an EDS1-NRG1-
277 SAG101 module to regulate downstream events in TNL immunity. To test this further,
278 higher order mutants combining loss-of-function mutations from different modules were
279 generated in *snc1* background. The dwarfism and increased *PR1* (*Pathogenesis-Related*
280 *1*) gene expression of *snc1* was partially suppressed by introducing mutations in *SAG101*
281 (Feys et al., 2005) or *NRG1* cluster (Wu et al., 2019) (Figure 4A-B). However, *snc1*
282 *sag101-1 nrg triple* resembled the *snc1 sag101-1* and *snc1 nrg triple* in morphology
283 (Figure 4A) and *PR1* gene expression levels (Figure 4B), confirming that SAG101 works
284 in the same pathway as NRG1A/1B. In contrast, the increased *PR1* gene expression of
285 *snc1* was largely, but not fully, suppressed by *adr1 triple* or *pad4-1* (Figure 4B), although
286 the size of *snc1 adr1 triple* and *snc1 pad4-1* was WT like (Cheng et al., 2011; Dong et
287 al., 2016) (Figure 4A). However, combining *adr1 triple* and *pad4* mutations together did
288 not further reduce the *PR1* gene expression (Figure 4B and S7), confirming that ADR1s
289 and PAD4 work in the same pathway. In contrast, mutants containing mutations in two
290 components from different modules, including *snc1 pad4-c1 sag101-1*, *snc1 pad4-c1 nrg*
291 *triple*, *snc1 sag101-c1 adr1 triple*, *snc1 adr1 triple nrg triple*, exhibited fully restored
292 WT-like levels of *PR1* expression (Figure 4A-B and S7). Taken together, these epistasis
293 analyses data confirm that two distinct modules are present in TNL pathways that act in
294 parallel, one includes PAD4-ADR1s and the other includes SAG101-NRG1A/1B.
295
296 To examine the relationship between NRG1C and the NRG1-SAG101 module, *NRG1C*
297 was overexpressed in the *snc1 nrg triple* or *snc1 sag101-1* background. As shown in
298 Figure 4C, the dwarfism was not further suppressed by *NRG1C* overexpression. In

299 agreement, *snc1 sag101-1 NRG1C OE* and *snc1 nrg triple NRG1C OE* resembled the
300 *snc1 sag101-1* and *snc1 nrg triple* in regards to *PR1* gene expression (Figure S8A).
301 Specifically, the increased *PR1* gene expression in *snc1* was reduced by either *nrg triple*
302 or *sag101*, but not further by *NRG1C* overexpression (Figure S8A). In contrast, the
303 partial suppression of up-regulated *PR1* gene expression in *snc1* by *adr1 triple* or *pad4-1*
304 was further suppressed to WT levels when *NRG1C* was overexpressed in *snc1 adr1 triple*
305 or *snc1 pad4-1* backgrounds (Figure S8B). These comprehensive epistasis data support
306 that NRG1C indeed specifically antagonizes the NRG1-SAG101 module.
307
308 **_NRG1C_ does not impact _NRG1A/1B_ through transcriptional interference**
309
310 As *NRG1C* encodes a truncated hNLR and works antagonistically with the SAG101-
311 NRG1 module, we first hypothesized that it might interfere with *NRG1A/1B* transcription
312 through RNA-mediated interference due to their sequence similarity. To test this, *NRG1C*
313 with a premature stop codon at position 213 of the predicted *NRG1C* mRNA sequence
314 was overexpressed in *chs3-2D* background. Such a mutation would yield a non-functional
315 protein $NRG1C^{T71*}$ but a rather normal transcript. No alterations in *chs3-2D*-mediated
316 dwarfism (Figure 5A-C) and enhanced disease resistance to *H.a.* Noco2 (Figure 5D) were
317 observed by overexpression of $NRG1C^{T71*}$ (Figure 5B), suggesting that NRG1C does not
318 affect mRNA levels of the full-length helper *NRG1A/1B*. Thus, if NRG1C interferes with
319 NRG1A/1B, the effects are likely protein-related.
320
321 **NRG1C antagonizes NRG1A-mediated defense and HR**
322

323 To further examine the hypothesis that NRG1C might directly interfere with NRG1A/1B,
324 we overexpressed *NRG1C* in autoimmune transgenic plants expressing *NRG1A D485V*,
325 an auto-active version of NRG1A that constitutively activates immunity (Wu et al.,
326 2019). The dwarfism and enhanced resistance of *NRG1A D485V* were largely suppressed
327 upon *NRG1C* overexpression (Figure 6A-B and S9A), while no effect on NRG1A protein
328 level was observed (Figure 6C). These results further support that the negative regulation
329 of NRG1A by NRG1C is not through transcriptional or post-transcriptional repression.
330
331 Consistent with our observation in *A. thaliana*, NRG1A D485V-triggered HR in *N.*
332 *benthamiana* was alleviated when co-expressed with NRG1C (Figure S9B-C), although
333 the same amount of NRG1A D485V proteins accumulated (Figure S9D). However,
334 overexpression of *NRG1C* did not alter the autoimmunity of *ADR1-L2 D484V*, an auto-
335 active variant of ADR1-L2 (Roberts et al., 2013) (Figure S10A-C). Taken together, these
336 data indicate that NRG1A-mediated autoimmunity and HR are negatively regulated by
337 NRG1C and the effects of NRG1C seem to be specific to NRG1-type hNLR-mediated
338 defense responses.
339
340 **NRG1C does not associate with full-length NRG1A**
341
342 Since NRG1C does not affect the mRNA or protein levels of full-length NRG1A, another
343 hypothesis is that NRG1C might interfere with NRG1A/1B through protein-protein
344 interactions. The recently developed TurboID-based proximity labeling method allows
345 TurboID-fused protein to biotinylate proximal and interacting proteins in the presence of
346 biotin *in vivo* (Zhang et al., 2019). This unbiased method can more reliably detect weak

347 and transient protein-protein interactions. When NRG1A-HA-TurboID was co-expressed
348 with NRG1C-3FLAG in the presence of RBA1, which induces NRG1 dependent
349 immunity (Figure S11A) (Qi et al., 2018; Wan et al., 2019), biotinylated NRG1C-3FLAG
350 was not detected despite the fact that NRG1C-3FLAG protein was significantly enriched
351 (Figure S11B). This negative interaction result suggests that the NRG1C-mediated
352 negative regulation of NRG1A-mediated defense may not be through direct protein
353 interference. However, we cannot exclude the possibility that the *in planta* interactions
354 between the two proteins could not be detected due to low protein expression or complex
355 conformation constraints.
356
357 **NRG1C associates with the EDS1-SAG101 complex**
358 As *NRG1C* overexpression also shares similar phenotypes with the *sag101* knockouts, we
359 then tested whether NRG1C could interfere with NRG1A-mediated defense by
360 associating with SAG101 or its constitutively associated partner EDS1. When *N.*
361 *benthamiana* leaves were infiltrated with *Agrobacterium* expressing EDS1-HA-TurboID,
362 NRG1C-3FLAG and SAG101-3FLAG, both IP-enriched SAG101-3FLAG and NRG1C-
363 3FLAG were biotinylated (Figure S12A). This suggests that basal levels of NRG1C
364 proteins are in close proximity to the C-terminus of EDS1, where the TurboID was fused.
365 In comparison, in *N. benthamiana* leaves pre-infiltrated with *Agrobacterium* harboring
366 RBA1, a similar amount of IP-enriched SAG101-3FLAG, but relatively more NRG1C-
367 3FLAG, was biotinylated by EDS1-HA-TurboID (Figure 6D, Figure S12A and Figure
368 S14C), suggesting that TNL activation likely enhances the association between NRG1C
369 and the EDS1-SAG101 complex. Interestingly, when this TurboID-mediated proximity

370 labeling assay was performed in the absence of SAG101-3FLAG, biotinylated NRG1C
371 was no longer detected (Figure S12B), indicating that the association between EDS1 and
372 SAG101 is needed to retain NRG1C in the complex.
373
374 We further examined such interaction with a reciprocal TurboID-based proximity
375 labeling assay using *A. thaliana* stable transgenic lines carrying both *NRG1C-HA-*
376 *TurboID* and *SAG101-3FLAG*. Transgenic plants were pretreated with *Agrobacterium*
377 expressing RBA1 and whole seedling plants were harvested at 6 hpi. As shown in Figure
378 6E, although NRG1C-HA-TurboID could not be observed in the SAG101-3FLAG pull-
379 down likely due to its low protein abundance, NRG1C-HA-TurboID successfully
380 biotinylated SAG101-3FLAG, but not EDS1, even though a large amount of EDS1
381 protein was pulled down. This suggests that SAG101 is in close proximity with the C-
382 terminus of NRG1C, where TurboID is fused. In addition, neither EDS1 (Figure S13A-B)
383 nor SAG101 (Figure S13C-D) protein levels were altered by *NRG1C* overexpression,
384 confirming that NRG1C does not affect the protein levels of the EDS1-SAG101-
385 NRG1A/1B module.
386
387 TIR domains of many TNLs exhibit nicotinamide adenine dinucleotide (NAD^+)
388 hydrolase (NADase) activity, with a conserved catalytic glutamic acid (Horsefield et al.,
389 2019; Wan et al., 2019). The catalytically dead $RBA1_{E86A}$ mutant retains self-association,
390 but fails to trigger cell death *in planta* (Wan et al., 2019). To test whether the association
391 between NRG1C and the EDS1-SAG101 complex is influenced by the TIR NADase
392 activity, *N. benthamiana* leaves expressing EDS1-HA-TurboID, SAG101-3FLAG and

393 NRG1C-3FLAG were pretreated with *Agrobacterium* expressing $RBA1_{E86A}$ mutant. As
394 shown in Figure S14A and S14C, SAG101-3FLAG and basal levels of NRG1C-3FLAG
395 were biotinylated by EDS1-HA-TurboID, suggesting that TIR NADase enzyme activity
396 is required for TNL-enhanced high order complex formation.
397
398 As EDS1 also constitutively interacts with PAD4, we also tested whether NRG1C
399 associates with the EDS1-PAD4 complex. However, when *N. benthamiana* leaves were
400 infiltrated with *Agrobacterium* expressing EDS1-HA-TurboID, NRG1C-3FLAG and
401 PAD4-ZZ-TEV-FLAG in the presence of RBA1 induction, EDS1-HA-TurboID was able
402 to label PAD4-ZZ-TEV-FLAG, but not NRG1C-3FLAG (Figure S14B). This specificity
403 of NRG1C with SAG101 explains why NRG1C explicitly antagonizes EDS1-SAG101-
404 NRG1 module-dependent immunity. It is worth noting that *N. benthamiana* contains its
405 own copies of *NRG1*, *SAG101* and *EDS1*. NbSAG101 is apparently not sufficient to
406 induce proximity between AtEDS1 and AtNRG1C (Figure S12B and S14B). This is
407 consistent with previous findings that lipase-like proteins (EDS1, PAD4, and SAG101)
408 and hNLRs (ADR1s and NRG1s) can only signal together when they come from the
409 same species (Lapin et al., 2019).

410 **Overexpression of *B. rapa* NRG1C ortholog suppresses *chs3-2D*-mediated defense**
411
412 As the presence of *NRG1C*-type N-terminally truncated hNLRs in *NRG1* clusters seems
413 to be a singular event in the evolution of Brassicaceae, we further tested whether they are
414 functionally transferable among different Brassicaceae species. To test this,
415 *Brara.I00877.1* (*BraNRG1C*) was overexpressed in the *chs3-2D* mutant. Consistent with
416 the phylogeny that Brassicaceae NRG1C family arose from a common ancestor (Figure

417 1A), overexpression of *BraNRG1C* fully rescued the *chs3-2D*-mediated dwarfism (Figure
418 7A-C) and enhanced disease resistance to *H.a.* Noco2 (Figure 7D). Taken together,
419 NRG1C function seems to be conserved in Brassicaceae species.
420

421 **NbNRG2 negatively regulates HopQ1-1-mediated immunity in *N. benthamiana***
422

423 To further explore further the function of truncated NRG1C outside the Brassicaceae, we
424 examined *N. benthamiana* NRG2 (NbNRG2) in HopQ1-1-mediated NRG1-dependent
425 ROQ1 (RECOGNITION of XopQ 1) resistance (Qi et al., 2018; Schultink et al., 2017)
426 (Figure S15A). Interestingly, overexpression of *NbNRG2* (Figure S15B) could suppress
427 HopQ1-1-mediated HR, which was induced by *P.s.t.* CUCPB5500 HopQ1-1 (Figure 7E
428 and G). By contrast, the HopQ1-1-mediated HR was not suppressed by overexpression
429 of Brassicaceae orthologs including *A. thaliana NRG1C* (Figure 7F and H; Figure S15C)
430 or *BraNRG1C* (Figure S15D-F), indicating that these Brassicaceae orthologs are not able
431 to inhibit *N. benthamiana* TNL ROQ1-mediated immunity. Furthermore, overexpression
432 of *NbNRG2* (Figure S16B) failed to suppress *chs3-2D*-mediated dwarfism (Figure S16A
433 and C) and enhanced disease resistance to *H.a.* Noco2 (Figure S16D). Since molecular
434 incompatibility among different species or clades was observed in the EDS1-SAG101-
435 NRG1 module (Lapin et al., 2019), it is not surprising that NbNRG2 and Brassicaceae
436 NRG1Cs are not functionally exchangeable and their negative regulation requires
437 molecular compatibility.
438

439 **Discussion**
440

441 Truncated NLRs, including TIR only, TN, TIR-unknown domain (TX), CC only, CC-NB
442 (CN), CC-unknown domain (CX), RPW8 only, RPW8-NB (RN), NB-LRR (NL), NB
443 only and LRR only, are commonly found encoded in the genomes of higher plants
444 (Baggs et al., 2017; Bai et al., 2002; Jacob et al., 2013; Lee and Chae, 2020; Meyers et
445 al., 2003; Meyers et al., 2002; Nandety et al., 2013; Van de Weyer et al., 2019; Yang et
446 al., 2008). A genome-wide survey of *A. thaliana* NLR genes revealed that around 31% of
447 NLR genes are truncated (Meyers et al., 2003). Among them, approximately 90% lack
448 canonical C-terminal domains (Meyers et al., 2003; Meyers et al., 2002). Functional
449 characterizations of some C-terminally truncated NLRs have been reported. The TIR-
450 only protein RBA1 can function as an effector sensor and trigger plant immune responses
451 by self-oligomerization (Nishimura et al., 2017). Moreover, the TIR domain in the RBA1
452 protein possesses NADase activity, which is required to trigger cell death (Wan et al.,
453 2019). Other well-studied TN proteins include TN2 and CHS1. TN2 guards the exocyst
454 complex subunit EXO70B1 (Zhao et al., 2015) and may stabilize active calcium-
455 dependent protein kinase CPK5 to regulate defense responses (Liu et al., 2017).
456 Interestingly, *TNL SOC3* and *CHS1* cluster together with *TN2* (Liang et al., 2019; Zhang
457 et al., 2017). SOC3 pairs with either CHS1 or TN2 to monitor the absence or
458 overaccumulation of E3 ligase SAUL1 (Liang et al., 2019; Tong et al., 2017). A recent
459 study found that LRR-PL (Post-LRR) truncated protein $DM10^{TueScha-9}$ (DANGEROUS
460 MIX 10) shows an incompatible interaction with $DM11^{Cdm-0}$ (DANGEROUS MIX 11),
461 resulting in hybrid necrosis (Barragan et al., 2020). Therefore, the C-terminally truncated
462 NLRs often can still serve positive roles in NLR activation, as they retain the N-terminal
463 signaling domains such as the TIR and NB regions.

464 In contrast, about 10% of truncated NLRs are N-terminally truncated in *A. thaliana*
465 (Meyers et al., 2003). Although they are widely present in all higher plant genomes, little
466 is known about their biological significance. In mammalian system, the TLR (Toll-like
467 receptors) TIR truncations can act as dominant-negative (DN) proteins to dampen
468 immune responses by associating with the same immune activation complexes (Burns et
469 al., 2003; Padmanabhan et al., 2009; Wells et al., 2006). Here, similar to the truncated
470 TLRs, the N-terminally truncated helper NRG1C lacking the RPW8 CC and part of the
471 NB domain can negatively regulate NRG1A/1B-mediated defense responses. Compared
472 to the DN-TLR examples in the mammalian system, how exactly NRG1C interferes with
473 NRG1A/1B signaling is less clear. As overexpression of a *NRG1C* variant containing a
474 premature stop codon failed to suppress *chs3-2D*-mediated autoimmunity, the mechanism
475 is unlikely to be due to transcriptional interference (Figure 5). Additionally, NRG1A-HA-
476 TurboID was unable to label NRG1C-3FLAG even in the presence of an elicitor,
477 suggesting that NRG1C does not interact with NRG1A/1B, although caution should
478 always be taken with negative protein-protein interaction data. However, NRG1C is in
479 close proximity with the EDS1-SAG101 complex, and this association seems to be
480 enhanced with TNL-induction (Figure 6D-E, Figure S12A-B and Figure S14C). To our
481 delight, our observation was recently independently supported by a SAG101-YFP IP-MS
482 (Immunoprecipitation Mass-Spectrometry) analysis, where peptides of NRG1C were
483 abundantly observed in immuno-precipitates of SAG101-YFP upon *Pf0-1 avrRPS4*
484 treatment (Figure 3a and Figure s5a, Sun et al., 2020). More peptides from NRG1C were
485 present in the SAG101 IP than the ones from NRG1A/1B, corroborating the interaction
486 between NRG1C and EDS1-SAG101. Additionally, Sun *et al.,* also found that NRG1A

487 associates with the EDS1-SAG101 dimer in an effector-dependent manner. Therefore,
488 NRG1C possibly antagonizes NRG1A/1B signaling by interfering with the EDS1-
489 SAG101 dimer. It seems that upon infection, a large complex consisting of EDS1,
490 NRG1A/1B and SAG101 forms, and NRG1C likely acts by interfering with such
491 complex assembly to avoid aberrant activation (Figure 7I). NRG1C may occupy the
492 NRG1A/1B space in the EDS1-SAG101-NRG1 complex, preventing NRG1A/1B
493 interaction with the lipase-like proteins. This explains the negative interaction data
494 between NRG1A and NRG1C. Further biochemical and structural analyses of these
495 proteins are needed to clarify the details of these interactions.

496

497 Both NRG1C and ADR1-L3 are N-terminally truncated hNLRs. Although NRG1C
498 negatively regulates some TNL-mediated defense, no effect on ADR1-dependent TNL
499 mediated autoimmunity or pathogen growth was observed upon *ADR1-L3* overexpression
500 (Figure S4A-C). In contrast to NRG1C, ADR1-L3 retains the full NB domain (Figure S1
501 and S3). NRG1C orthologs are commonly found in Brassicaceae (Figure 1A), whereas
502 ADR1-L3 ortholog is only present in *Boechera stricta* (Figure S3). Such an evolutionary
503 difference indicates that ADR1-L3 is likely a pseudogene and thus was lost during
504 evolution. Therefore, for N-terminally truncated NLRs in higher plant genomes, some
505 may be pseudogenes, and some may have negative functions as with NRG1C. Although
506 an evolutionary examination may provide an initial hint, functional analysis is needed to
507 determine their exact roles.

508

509 Besides NRG1C and ADR1-L3, five additional N-terminally truncated *NB-LRR* genes are
510 present in the *A. thaliana* Col-0 genome (Table S2). AT4G19050, AT5G45510 and
511 AT1G61300 are more closely related to CNLs (Meyers et al., 2003). *AT4G19050* is
512 adjacent to a CN gene *AT4G19060*. *AT5G45510* and head-to-head arranged CNL
513 *AT5G45520* form a cluster with two other CN genes *AT5G45490* and *AT5G45440*.
514 *AT1G61310* and adjacent CNL *AT1G61300*, are transcribed in the same direction (Table
515 S2). Only two NL proteins, AT5G38350 and AT4G09360, share a similar NB motif with
516 TNLs. *AT5G38350* clusters together with TIR-only gene *AT5G38344* and TNL gene
517 *AT5G38340*, while *AT4G09360* resides in the TNL cluster containing TNL *AT4G09430*
518 and *AT4G09420* (Table S2). Therefore, clustering of *NL* genes with full-length or C-
519 terminally truncated sNLRs can also be detected in *A. thaliana*. It is possible that the*NL*
520 genes in these clusters plays a similar role as *NRG1C* in the *NRG1* cluster, serving
521 negative regulatory functions. Additional investigations into the functions of such *NL*
522 genes in *A. thaliana* and other plants will be of great interest to widen our understanding
523 of NLRs.

524

525 **Materials and Methods**

526 **Plant growth conditions**

527 *A. thaliana* and *N. benthamiana* plants were grown at 22ºC under 16hr light/8hr dark
528 regime, unless otherwise specified. Severe autoimmune mutants were grown at 28 ºC to
529 suppress the dwarfism and enable seed production.

530 **Construction of plasmids**

531 Overexpression construct of *NRG1C* was made in *pCambia1305* vector. $NRG1C^{T71*}$ was
532 cloned into *pCambia1305* vector as well. The overexpression construct of *NRG1C* in
533 *NRG1A D485V* was cloned into *pBASTA* vector. The overexpression constructs of
534 *BraNRG1C* and *NbNRG2* were cloned into *pBASTA* vector by using the extracted

genomic DNA from *Brassica napus L.* cv. *Westar* and *N. benthamiana*. *DAR5* was cloned into *pHan* vector. For the TurboID-based proximity labeling assay, *NRG1A* and *EDS1* were cloned into *pBASTA-HA-TurboID*. *NRG1C* was cloned into *pCambia1305-3FLAG*. *pBASTA NRG1A-3FLAG* and *pCambia1300 EDS1-3FLAG* were described in previous studies (Wu et al., 2019).

To generate the CRISPR/Cas9 constructs for knocking out *PAD4* and *SAG101*, genomic sequences of *PAD4* and *SAG101* were subjected to CRISPRscan (http://www.crisprscan.org/?page=sequence) to identify the target sequences. The selected sequences were evaluated with Cas-OFFinder (http://www.rgenome.net/cas-offinder/). The pHEE401E vector was used to generate the CRISPR/Cas9 constructs following the protocols previously described (Wang et al., 2015). All primers used are listed in Supplemental Table 3.

A. thaliana stable transformation

The binary constructs were introduced into *Agrobacterium tumefaciens* GV3101 by electroporation and subsequently transformed into *A. thaliana* by the floral dipping method (Clough and Bent, 1998). For *snc1*, *chs1-2* and *chs2-1* transformation, plants were grown at room temperature. For *chs3-2D* transformation, plants were grown at 28ºC under 16hr light/8hr dark regime to reduce autoimmunity. Transformants were selected either on soil by spraying BASTA (Glufosinate ammonium) or on plates with Hygromycin B. 10 transformants were selected each and co-segregation analysis in T2 generations were carried out to make sure the suppression phenotypes were due to the transgene overexpression.

Transient *N. benthamiana* expression

Transient *N. benthamiana* expression assays were performed as previously described (Wu et al., 2017b). In brief, *Agrobacteria* carrying the respective constructs were co-infiltrated into four-week-old *N. benthamiana* leaves. Final OD_{600} for most strains was 0.2, whereas OD_{600} =1.0 and 0.6 were used for all strains expressing NRG1C or SAG101, respectively. Each infiltration contained *Agrobacteria* expressing *p19* to inhibit gene silencing (Lakatos et al., 2004).

Pathogen infections

Oomycete and bacterial pathogen infection assays were carried out as described previously (Li et al., 2001). In brief, two-week-old soil-grown seedlings were sprayed with *H.a.* Noco2 or Emwa1 conidia spores at a concentration of 10^5 spores per ml water. Sporulation was quantified using a hemocytometer after plants were grown at 18°C for 7 days. For bacterial infections, four-week-old plants were infiltrated with bacterial solution at designated concentrations. Leaf discs were collected and ground on the day of infection (Day 0) and 3 days later (Day 3). Colony-forming units (cfu) were calculated after incubation on LB plates with appropriate antibiotic selection. For HR assay in *A. thaliana*, four-week-old soil-grown plants were hand infiltrated with *Pf0-1* carrying pBS46:AvrRPS4. Cell death was monitored at 36 hpi.

575 **Expression analysis**

576 About 0.05 g of four-week-old soil-grown plant tissue was collected, and RNA was
577 extracted using an RNA isolation kit (Bio Basic; Cat#BS82314). ProtoScript II reverse
578 transcriptase (NEB; Cat#B0368) was used to generate cDNA. Real-time PCR was
579 performed using a SYBR premix kit (TaKaRa, Cat#RR82LR). The primers used are
580 listed in Supplemental Table 3.

581 ***Agrobacteria* infiltration following *P.s.t.* CUCPB5500 HopQ1-1 infection**

582 *Agrobacteria* carrying the respective constructs were infiltrated into four-week-old *N.*
583 *benthamiana* leaves. *P.s.t.* CUCPB5500 HopQ1-1 was then infiltrated in the indicated
584 area 48 hrs after *Agrobacteria* infiltration. Ion leakage was measured at 4 days after *P.s.t.*
585 CUCPB5500 HopQ1-1 infection.

586 **Ion leakage measurement in *N. benthamiana***

587 After agrobacteria infiltration and *P.s.t.* CUCPB5500 HopQ1-1 infection, leaf discs from
588 *N. benthamiana* were collected and washed in 10 ml of milliQ water overnight at room
589 temperature. Ion leakage was measured with a conductometer VWR E C METER Model
590 2052. All samples were then autoclaved to measure the total ion leakage.

591 **TurboID-based proximity labeling in *N. benthamiana***

592 TurboID-based proximity labeling assay was performed as described previously (Wu et
593 al., 2020; Zhang et al., 2019). In brief, *N. benthamiana* leaves were infiltrated with
594 agrobacteria containing *HA-TurboID* and *3FLAG* tagged constructs. At 48 hpi,
595 agrobacteria expressing RBA1 or $RBA1_{E86A}$ constructs were infiltrated (Wan et al.,
596 2019). At 52 hpi, biotin was infiltrated, and the plants were incubated at room
597 temperature for 2 h to allow labeling. Leaves were harvested, followed by
598 immunoprecipitation and western blot analysis.

599 **TurboID-based proximity labeling in *Arabidopsis***

600 Two-week-old plate-grown *Arabidopsis* transgenic lines carrying both *NRG1C-HA-*
601 *TurboID* and *SAG101-3FLAG* were soaked with *Agrobacteria* expressing RBA1
602 (OD_{600}=0.2). At 4 hpi, biotin was added in solution and the plants were incubated at room
603 temperature for 2 hours for labeling. The plants were then harvested, followed by
604 immunoprecipitation and western blot analysis.

605 **Protein extraction, immunoprecipitation, and western blot analysis**

606 100 mg soil-grown *A. thaliana* plant leaves or *N. benthamiana* leaves were collected and
607 extracted by extraction buffer (100 mM Tris-HCl pH 8.0, 0.2% SDS and 2% β-
608 mercaptoethanol). Loading buffer was added to each protein sample and boiled for 5 min.
609 Protein abundance was quantified using ImageJ (https://imagej.nih.gov/ij/).

610 Co-immunoprecipitation assay was performed as previously described (Wu et al., 2017b).
611 In brief, *N. benthamiana* plants were infiltrated with agrobacteria. About 2.5 g *N.*

612 *benthamiana* leaves expressing the indicated proteins were harvested at 54 hpi and
613 ground into powder with liquid nitrogen. Extraction buffer contains 25 mM Tris-HCl pH
614 7.5, 150 mM NaCl, 1mM EDTA, 0.15% Nonidet P-40, 10% Glycerol, 1 mM PMSF, 1×
615 Protease Inhibitor Cocktail (Roche; Cat. #11873580001), and 10 mM DTT. The FLAG-
616 tagged NRG1C and SAG101 proteins were immunoprecipitated using 20 µl M2 beads
617 (Sigma; Cat. #A2220) for co-immunoprecipitation and biotinylation was detected by
618 Streptavidin-HRP (Abcam Cat. # ab7403)

619 The anti-HA antibody was from Roche (Cat. #11867423001). The anti-FLAG antibody
620 was from Sigma (Cat. #F1804). The anti-EDS1 antibody was generously shared from Dr.
621 Jane E. Parker (Feys et al., 2001).

622 **Statistical analysis**

623 One-way ANOVA followed by Tukey's post hoc test was performed. The Scheffé
624 multiple comparison was applied for testing correction. Normality test for all data was
625 done in SPSS. Statistical significance was indicated with different letters. *p* values and
626 sample numbers (n) were detailed in figure legends.

627 **Acknowledgments**

628 Drs. Jeff Dangl, Jane Parker, Brian Staskawicz, Pingtao Ding, Jonathan Jones, Yu Ti
629 Cheng and Shenyang He are cordially thanked for generous sharing of *A. thaliana* seeds
630 of mutants, anti-EDS1 antibody and *Pseudomonas Avr* strains. Dr. Marc T. Nishimura is
631 thanked for sharing the RBA1 constructs. Dr. Brian J. Staskawicz is thanked for sharing
632 the *nrg1-1 N. benthamiana* seeds. Mr. Kevin Ao and Dr. Paul Kapos are sincerely
633 thanked for careful reading of the manuscript. This work was financially supported by
634 CFI-JELF, the Natural Sciences and Engineering Research Council of Canada (NSERC)
635 Discovery Program, NSERC-CREATE PRoTECT program, and the WD Cooper
636 Memorial Fund from UBC.

637 **Author contributions**

638 ZW, Data curation, Validation, Investigation, Methodology, Writing - original draft,
639 Project administration; LT, Validation, Methodology; X Li, Conceptualization, Data
640 curation, Formal analysis, Supervision, Funding acquisition, Writing—original draft,
641 Project administration, Writing - revisions. All authors reviewed the manuscript.
642

643 **Conflict of interest**

644 Nothing declared.

645

646 **References**

647 Adachi, H., Contreras, M.P., Harant, A., Wu, C.H., Derevnina, L., Sakai, T., Duggan, C., Moratto,
648 E., Bozkurt, T.O., Maqbool, A., et al. (2019). An N-terminal motif in NLR immune
649 receptors is functionally conserved across distantly related plant species. Elife 8.

650 Andolfo, G., Villano, C., Errico, A., Frusciante, L., Carputo, D., Aversano, R., and Ercolano, M.R.
651 (2019). Inferring RPW8-NLRs's evolution patterns in seed plants: case study in Vitis
652 vinifera. Planta 251:32.
653 Baggs, E., Dagdas, G., and Krasileva, K.V. (2017). NLR diversity, helpers and integrated domains:
654 making sense of the NLR IDentity. Curr Opin Plant Biol 38:59-67.
655 Bai, J., Pennill, L.A., Ning, J., Lee, S.W., Ramalingam, J., Webb, C.A., Zhao, B., Sun, Q., Nelson, J.C.,
656 Leach, J.E., et al. (2002). Diversity in nucleotide binding site-leucine-rich repeat genes in
657 cereals. Genome Res 12:1871-1884.
658 Barragan, A.C., Collenberg, M., Wang, J., Lee, R.R.Q., Cher, W.Y., Rabanal, F.A., Ashkenazy, H.,
659 Weigel, D., and Chae, E. (2020). A truncated singleton NLR causes hybrid necrosis in
660 Arabidopsis thaliana. Mol Biol Evol.
661 Bonardi, V., Tang, S., Stallmann, A., Roberts, M., Cherkis, K., and Dangl, J.L. (2011). Expanded
662 functions for a family of plant intracellular immune receptors beyond specific
663 recognition of pathogen effectors. Proc Natl Acad Sci U S A 108:16463-16468.
664 Burns, K., Janssens, S., Brissoni, B., Olivos, N., Beyaert, R., and Tschopp, J. (2003). Inhibition of
665 interleukin 1 receptor/Toll-like receptor signaling through the alternatively spliced, short
666 form of MyD88 is due to its failure to recruit IRAK-4. J Exp Med 197:263-268.
667 Castel, B., Ngou, P.M., Cevik, V., Redkar, A., Kim, D.S., Yang, Y., Ding, P., and Jones, J.D.G. (2019).
668 Diverse NLR immune receptors activate defence via the RPW8-NLR NRG1. New Phytol
669 222:966-980.
670 Cheng, Y.T., Li, Y., Huang, S., Huang, Y., Dong, X., Zhang, Y., and Li, X. (2011). Stability of plant
671 immune-receptor resistance proteins is controlled by SKP1-CULLIN1-F-box (SCF)-
672 mediated protein degradation. Proc Natl Acad Sci U S A 108:14694-14699.
673 Clough, S.J., and Bent, A.F. (1998). Floral dip: a simplified method for Agrobacterium-mediated
674 transformation of Arabidopsis thaliana. Plant J 16:735-743.
675 Collier, S.M., Hamel, L.P., and Moffett, P. (2011). Cell death mediated by the N-terminal domains
676 of a unique and highly conserved class of NB-LRR protein. Mol Plant Microbe Interact
677 24:918-931.
678 Couto, D., and Zipfel, C. (2016). Regulation of pattern recognition receptor signalling in plants.
679 Nat Rev Immunol 16:537-552.
680 Cui, H., Tsuda, K., and Parker, J.E. (2015). Effector-triggered immunity: from pathogen
681 perception to robust defense. Annu Rev Plant Biol 66:487-511.
682 Dong, O.X., Tong, M., Bonardi, V., El Kasmi, F., Woloshen, V., Wünsch, L.K., Dangl, J.L., and Li, X.
683 (2016). TNL-mediated immunity in Arabidopsis requires complex regulation of the
684 redundant ADR1 gene family. New Phytol 210:960-973.
685 Feys, B.J., Moisan, L.J., Newman, M.A., and Parker, J.E. (2001). Direct interaction between the
686 Arabidopsis disease resistance signaling proteins, EDS1 and PAD4. EMBO J 20:5400-
687 5411.
688 Feys, B.J., Wiermer, M., Bhat, R.A., Moisan, L.J., Medina-Escobar, N., Neu, C., Cabral, A., and
689 Parker, J.E. (2005). Arabidopsis SENESCENCE-ASSOCIATED GENE101 stabilizes and
690 signals within an ENHANCED DISEASE SUSCEPTIBILITY1 complex in plant innate
691 immunity. Plant Cell 17:2601-2613.
692 Gabriëls, S.H., Takken, F.L., Vossen, J.H., de Jong, C.F., Liu, Q., Turk, S.C., Wachowski, L.K., Peters,
693 J., Witsenboer, H.M., de Wit, P.J., et al. (2006). CDNA-AFLP combined with functional
694 analysis reveals novel genes involved in the hypersensitive response. Mol Plant Microbe
695 Interact 19:567-576.
696 Gabriëls, S.H., Vossen, J.H., Ekengren, S.K., van Ooijen, G., Abd-El-Haliem, A.M., van den Berg,
697 G.C., Rainey, D.Y., Martin, G.B., Takken, F.L., de Wit, P.J., et al. (2007). An NB-LRR protein

698 required for HR signalling mediated by both extra- and intracellular resistance proteins.
699 Plant J 50:14-28.
700 Gao, Y., Wang, W., Zhang, T., Gong, Z., Zhao, H., and Han, G.Z. (2018). Out of Water: The Origin
701 and Early Diversification of Plant. Plant Physiol 177:82-89.
702 Guo, Y.L., Fitz, J., Schneeberger, K., Ossowski, S., Cao, J., and Weigel, D. (2011). Genome-wide
703 comparison of nucleotide-binding site-leucine-rich repeat-encoding genes in
704 Arabidopsis. Plant Physiol 157:757-769.
705 Horsefield, S., Burdett, H., Zhang, X., Manik, M.K., Shi, Y., Chen, J., Qi, T., Gilley, J., Lai, J.S., Rank,
706 M.X., et al. (2019). NAD. Science 365:793-799.
707 Huang, X., Li, J., Bao, F., Zhang, X., and Yang, S. (2010). A gain-of-function mutation in the
708 Arabidopsis disease resistance gene RPP4 confers sensitivity to low temperature. Plant
709 Physiol 154:796-809.
710 Jacob, F., Vernaldi, S., and Maekawa, T. (2013). Evolution and Conservation of Plant NLR
711 Functions. Front Immunol 4:297.
712 Jones, J.D., Vance, R.E., and Dangl, J.L. (2016). Intracellular innate immune surveillance devices
713 in plants and animals. Science 354.
714 Jubic, L.M., Saile, S., Furzer, O.J., El Kasmi, F., and Dangl, J.L. (2019). Help wanted: helper NLRs
715 and plant immune responses. Curr Opin Plant Biol 50:82-94.
716 Krasileva, K.V. (2019). The role of transposable elements and DNA damage repair mechanisms in
717 gene duplications and gene fusions in plant genomes. Curr Opin Plant Biol 48:18-25.
718 Kvitko, B.H., Park, D.H., Velásquez, A.C., Wei, C.F., Russell, A.B., Martin, G.B., Schneider, D.J., and
719 Collmer, A. (2009). Deletions in the repertoire of Pseudomonas syringae pv. tomato
720 DC3000 type III secretion effector genes reveal functional overlap among effectors. PLoS
721 Pathog 5:e1000388.
722 Lakatos, L., Szittya, G., Silhavy, D., and Burgyán, J. (2004). Molecular mechanism of RNA silencing
723 suppression mediated by p19 protein of tombusviruses. EMBO J 23:876-884.
724 Lapin, D., Kovacova, V., Sun, X., Dongus, J.A., Bhandari, D., von Born, P., Bautor, J., Guarneri, N.,
725 Rzemieniewski, J., Stuttmann, J., et al. (2019). A Coevolved EDS1-SAG101-NRG1 Module
726 Mediates Cell Death Signaling by TIR-Domain Immune Receptors. Plant Cell 31:2430-
727 2455.
728 Lee, R.R.Q., and Chae, E. (2020). Variation Patterns of NLR Clusters in. Plant Commun 1:100089.
729 Li, X., Clarke, J.D., Zhang, Y., and Dong, X. (2001). Activation of an EDS1-mediated R-gene
730 pathway in the snc1 mutant leads to constitutive, NPR1-independent pathogen
731 resistance. Mol Plant Microbe Interact 14:1131-1139.
732 Liang, W., van Wersch, S., Tong, M., and Li, X. (2019). TIR-NB-LRR immune receptor SOC3 pairs
733 with truncated TIR-NB protein CHS1 or TN2 to monitor the homeostasis of E3 ligase
734 SAUL1. New Phytol 221:2054-2066.
735 Liu, N., Hake, K., Wang, W., Zhao, T., Romeis, T., and Tang, D. (2017). CALCIUM-DEPENDENT
736 PROTEIN KINASE5 Associates with the Truncated NLR Protein TIR-NBS2 to Contribute to.
737 Plant Cell 29:746-759.
738 Lu, X., Kracher, B., Saur, I.M., Bauer, S., Ellwood, S.R., Wise, R., Yaeno, T., Maekawa, T., and
739 Schulze-Lefert, P. (2016). Allelic barley MLA immune receptors recognize sequence-
740 unrelated avirulence effectors of the powdery mildew pathogen. Proc Natl Acad Sci U S
741 A 113:E6486-E6495.
742 Ma, S., Lapin, D., Liu, L., Sun, Y., Song, W., Zhang, X., Logemann, E., Yu, D., Wang, J., Jirschitzka,
743 J., et al. (2020). Direct pathogen-induced assembly of an NLR immune receptor complex
744 to form a holoenzyme. Science 370.

745 Mago, R., Zhang, P., Vautrin, S., Šimková, H., Bansal, U., Luo, M.C., Rouse, M., Karaoglu, H.,
746 Periyannan, S., Kolmer, J., et al. (2015). The wheat Sr50 gene reveals rich diversity at a
747 cereal disease resistance locus. Nat Plants 1:15186.
748 Marone, D., Russo, M.A., Laidò, G., De Leonardis, A.M., and Mastrangelo, A.M. (2013). Plant
749 nucleotide binding site-leucine-rich repeat (NBS-LRR) genes: active guardians in host
750 defense responses. Int J Mol Sci 14:7302-7326.
751 Martin, R., Qi, T., Zhang, H., Liu, F., King, M., Toth, C., Nogales, E., and Staskawicz, B.J. (2020).
752 Structure of the activated ROQ1 resistosome directly recognizing the pathogen effector
753 XopQ. Science 370.
754 Meyers, B.C., Kozik, A., Griego, A., Kuang, H., and Michelmore, R.W. (2003). Genome-wide
755 analysis of NBS-LRR-encoding genes in Arabidopsis. Plant Cell 15:809-834.
756 Meyers, B.C., Morgante, M., and Michelmore, R.W. (2002). TIR-X and TIR-NBS proteins: two new
757 families related to disease resistance TIR-NBS-LRR proteins encoded in Arabidopsis and
758 other plant genomes. Plant J 32:77-92.
759 Michelmore, R.W., and Meyers, B.C. (1998). Clusters of resistance genes in plants evolve by
760 divergent selection and a birth-and-death process. Genome Res 8:1113-1130.
761 Nandety, R.S., Caplan, J.L., Cavanaugh, K., Perroud, B., Wroblewski, T., Michelmore, R.W., and
762 Meyers, B.C. (2013). The role of TIR-NBS and TIR-X proteins in plant basal defense
763 responses. Plant Physiol 162:1459-1472.
764 Nishimura, M.T., Anderson, R.G., Cherkis, K.A., Law, T.F., Liu, Q.L., Machius, M., Nimchuk, Z.L.,
765 Yang, L., Chung, E.H., El Kasmi, F., et al. (2017). TIR-only protein RBA1 recognizes a
766 pathogen effector to regulate cell death in. Proc Natl Acad Sci U S A 114:E2053-E2062.
767 Padmanabhan, M., Cournoyer, P., and Dinesh-Kumar, S.P. (2009). The leucine-rich repeat
768 domain in plant innate immunity: a wealth of possibilities. Cell Microbiol 11:191-198.
769 Peart, J.R., Mestre, P., Lu, R., Malcuit, I., and Baulcombe, D.C. (2005). NRG1, a CC-NB-LRR
770 protein, together with N, a TIR-NB-LRR protein, mediates resistance against tobacco
771 mosaic virus. Curr Biol 15:968-973.
772 Qi, T., Seong, K., Thomazella, D.P.T., Kim, J.R., Pham, J., Seo, E., Cho, M.J., Schultink, A., and
773 Staskawicz, B.J. (2018). NRG1 functions downstream of EDS1 to regulate TIR-NLR-
774 mediated plant immunity in. Proc Natl Acad Sci U S A 115:E10979-E10987.
775 Rathjen, J.P., and Dodds, P.N. (2017). Dancing with the Stars: An Asterid NLR Family. Trends
776 Plant Sci 22:1003-1005.
777 Rietz, S., Stamm, A., Malonek, S., Wagner, S., Becker, D., Medina-Escobar, N., Vlot, A.C., Feys,
778 B.J., Niefind, K., and Parker, J.E. (2011). Different roles of Enhanced Disease
779 Susceptibility1 (EDS1) bound to and dissociated from Phytoalexin Deficient4 (PAD4) in
780 Arabidopsis immunity. New Phytol 191:107-119.
781 Roberts, M., Tang, S., Stallmann, A., Dangl, J.L., and Bonardi, V. (2013). Genetic requirements for
782 signaling from an autoactive plant NB-LRR intracellular innate immune receptor. PLoS
783 Genet 9:e1003465.
784 Saile, S.C., Jacob, P., Castel, B., Jubic, L.M., Salas-Gonzáles, I., Bäcker, M., Jones, J.D.G., Dangl,
785 J.L., and El Kasmi, F. (2020). Two unequally redundant "helper" immune receptor
786 families mediate Arabidopsis thaliana intracellular "sensor" immune receptor functions.
787 PLoS Biol 18:e3000783.
788 Saucet, S.B., Ma, Y., Sarris, P.F., Furzer, O.J., Sohn, K.H., and Jones, J.D. (2015). Two linked pairs
789 of Arabidopsis TNL resistance genes independently confer recognition of bacterial
790 effector AvrRps4. Nat Commun 6:6338.

791 Schultink, A., Qi, T., Lee, A., Steinbrenner, A.D., and Staskawicz, B. (2017). Roq1 mediates
792 recognition of the Xanthomonas and Pseudomonas effector proteins XopQ and HopQ1.
793 Plant J 92:787-795.
794 Serra, H., Choi, K., Zhao, X., Blackwell, A.R., Kim, J., and Henderson, I.R. (2018). Interhomolog
795 polymorphism shapes meiotic crossover within the Arabidopsis RAC1 and RPP13 disease
796 resistance genes. PLoS Genet 14:e1007843.
797 Shao, Z.Q., Xue, J.Y., Wu, P., Zhang, Y.M., Wu, Y., Hang, Y.Y., Wang, B., and Chen, J.Q. (2016).
798 Large-Scale Analyses of Angiosperm Nucleotide-Binding Site-Leucine-Rich Repeat Genes
799 Reveal Three Anciently Diverged Classes with Distinct Evolutionary Patterns. Plant
800 Physiol 170:2095-2109.
801 Sun, X., Lapin, D., Feehan, J., Stolze, S., Kramer, K., Dongus, J., Rzemieniewski, J., Blanvillain-
802 Baufumé, S., Harzen, A., Bautor, J., Derbyshire, P., Menke, F., Finkemeier, I., Nakagami,
803 H., Jones, JDG., and Parker, J.E.(2020). Pathogen effector recognition-dependent
804 association of NRG1 with EDS1 and SAG101 in TNL receptor immunity. bioRxiv.
805 Tamborski, J., and Krasileva, K.V. (2020). Evolution of Plant NLRs: From Natural History to Precise
806 Modifications. Annu Rev Plant Biol 71:355-378.
807 Tan, X., Meyers, B.C., Kozik, A., West, M.A., Morgante, M., St Clair, D.A., Bent, A.F., and
808 Michelmore, R.W. (2007). Global expression analysis of nucleotide binding site-leucine
809 rich repeat-encoding and related genes in Arabidopsis. BMC Plant Biol 7:56.
810 Thomas, W.J., Thireault, C.A., Kimbrel, J.A., and Chang, J.H. (2009). Recombineering and stable
811 integration of the Pseudomonas syringae pv. syringae 61 hrp/hrc cluster into the
812 genome of the soil bacterium Pseudomonas fluorescens Pf0-1. Plant J 60:919-928.
813 Tian, L., and Li, X. (2020). Enzyme formation by immune receptors. Science 370:1163-1164.
814 Tong, M., Kotur, T., Liang, W., Vogelmann, K., Kleine, T., Leister, D., Brieske, C., Yang, S., Lüdke,
815 D., Wiermer, M., et al. (2017). E3 ligase SAUL1 serves as a positive regulator of PAMP-
816 triggered immunity and its homeostasis is monitored by immune receptor SOC3. New
817 Phytol 215:1516-1532.
818 Van de Weyer, A.L., Monteiro, F., Furzer, O.J., Nishimura, M.T., Cevik, V., Witek, K., Jones, J.D.G.,
819 Dangl, J.L., Weigel, D., and Bemm, F. (2019). A Species-Wide Inventory of NLR Genes and
820 Alleles in Arabidopsis thaliana. Cell 178:1260-1272.e1214.
821 van Wersch, S., and Li, X. (2019). Stronger When Together: Clustering of Plant NLR Disease
822 resistance Genes. Trends Plant Sci 24:688-699.
823 Wan, L., Essuman, K., Anderson, R.G., Sasaki, Y., Monteiro, F., Chung, E.H., Osborne Nishimura,
824 E., DiAntonio, A., Milbrandt, J., Dangl, J.L., et al. (2019). TIR domains of plant immune
825 receptors are NAD. Science 365:799-803.
826 Wang, Y., Zhang, Y., Wang, Z., Zhang, X., and Yang, S. (2013). A missense mutation in CHS1, a
827 TIR-NB protein, induces chilling sensitivity in Arabidopsis. Plant J 75:553-565.
828 Wang, Z.P., Xing, H.L., Dong, L., Zhang, H.Y., Han, C.Y., Wang, X.C., and Chen, Q.J. (2015). Egg
829 cell-specific promoter-controlled CRISPR/Cas9 efficiently generates homozygous
830 mutants for multiple target genes in Arabidopsis in a single generation. Genome Biol
831 16:144.
832 Wells, C.A., Chalk, A.M., Forrest, A., Taylor, D., Waddell, N., Schroder, K., Himes, S.R., Faulkner,
833 G., Lo, S., Kasukawa, T., et al. (2006). Alternate transcription of the Toll-like receptor
834 signaling cascade. Genome Biol 7:R10.
835 Wicker, T., Yahiaoui, N., and Keller, B. (2007). Illegitimate recombination is a major evolutionary
836 mechanism for initiating size variation in plant resistance genes. Plant J 51:631-641.

837 Wu, C.H., Abd-El-Haliem, A., Bozkurt, T.O., Belhaj, K., Terauchi, R., Vossen, J.H., and Kamoun, S.
838 (2017a). NLR network mediates immunity to diverse plant pathogens. Proc Natl Acad Sci
839 U S A 114:8113-8118.
840 Wu, C.H., Belhaj, K., Bozkurt, T.O., Birk, M.S., and Kamoun, S. (2016). Helper NLR proteins
841 NRC2a/b and NRC3 but not NRC1 are required for Pto-mediated cell death and
842 resistance in Nicotiana benthamiana. New Phytol 209:1344-1352.
843 Wu, Z., Huang, S., Zhang, X., Wu, D., Xia, S., and Li, X. (2017b). Regulation of plant immune
844 receptor accumulation through translational repression by a glycine-tyrosine-
845 phenylalanine (GYF) domain protein. Elife 6.
846 Wu, Z., Li, M., Dong, O.X., Xia, S., Liang, W., Bao, Y., Wasteneys, G., and Li, X. (2019). Differential
847 regulation of TNL-mediated immune signaling by redundant helper CNLs. New Phytol
848 222:938-953.
849 Wu, Z., Tong, M., Tian, L., Zhu, C., Liu, X., Zhang, Y., and Li, X. (2020). Plant E3 ligases SNIPER1
850 and SNIPER2 broadly regulate the homeostasis of sensor NLR immune receptors. EMBO
851 J 39:e104915.
852 Xu, F., Zhu, C., Cevik, V., Johnson, K., Liu, Y., Sohn, K., Jones, J.D., Holub, E.B., and Li, X. (2015).
853 Autoimmunity conferred by chs3-2D relies on CSA1, its adjacent TNL-encoding
854 neighbour. Sci Rep 5:8792.
855 Yang, S., Zhang, X., Yue, J.X., Tian, D., and Chen, J.Q. (2008). Recent duplications dominate NBS-
856 encoding gene expansion in two woody species. Mol Genet Genomics 280:187-198.
857 Zbierzak, A.M., Porfirova, S., Griebel, T., Melzer, M., Parker, J.E., and Dörmann, P. (2013). A TIR-
858 NBS protein encoded by Arabidopsis Chilling Sensitive 1 (CHS1) limits chloroplast
859 damage and cell death at low temperature. Plant J 75:539-552.
860 Zhang, Y., Song, G., Lal, N.K., Nagalakshmi, U., Li, Y., Zheng, W., Huang, P.J., Branon, T.C., Ting,
861 A.Y., Walley, J.W., et al. (2019). TurboID-based proximity labeling reveals that UBR7 is a
862 regulator of N NLR immune receptor-mediated immunity. Nat Commun 10:3252.
863 Zhang, Y., Wang, Y., Liu, J., Ding, Y., Wang, S., Zhang, X., Liu, Y., and Yang, S. (2017).
864 Temperature-dependent autoimmunity mediated by chs1 requires its neighboring TNL
865 gene SOC3. New Phytol 213:1330-1345.
866 Zhao, T., Rui, L., Li, J., Nishimura, M.T., Vogel, J.P., Liu, N., Liu, S., Zhao, Y., Dangl, J.L., and Tang,
867 D. (2015). A truncated NLR protein, TIR-NBS2, is required for activated defense
868 responses in the exo70B1 mutant. PLoS Genet 11:e1004945.
869 Zhong, Y., and Cheng, Z.M. (2016). A unique RPW8-encoding class of genes that originated in
870 early land plants and evolved through domain fission, fusion, and duplication. Sci Rep
871 6:32923.

872 **Figure legends**
873

874 **Figure 1. *NRG1C* is evolutionarily conserved in Brassicaceae, and its transcription is**
875 **induced in TNL type autoimmune mutants and upon pathogen infection.**
876

877 A. Protein domain diagram of NRG1A, NRG1B and NRG1C. Numbers represent amino
878 acid positions relative to the translation start sites. NRG1C lacks the RPW8 CC and part
879 of the NB domains.
880

881 B. Phylogenetic tree of putative NRG1A/1B/1C orthologs. Putative NRG1A/1B/1C
882 orthologs were obtained from Phytozome (Brassicaceae species) and Sol Genomics
883 Network (*N. benthamiana*) using *A. thaliana* NRG1A, NRG1B and NRG1C protein
884 sequences as input, respectively. ZAR1 was used as an outgroup to root the tree.
885 MUSCLE was used for sequence alignment and a Neighbor-joining tree was generated
886 by using full-length NRG1C and homologous parts of all other corresponding NRG1
887 homologs with JTT model and using 2000 bootstrap replicates in MEGA 7.0.

888

889 C-D. *NRG1C* (C) and *DAR5* (D) gene expression in the autoimmune mutants *snc1* and
890 *chs3-2D* as determined by RT-PCR (Col-0 serves as wild type control and the transcript
891 level in Col-0 was arbitrarily set at 1.0). Statistical significance is indicated by different
892 letters ($p < 0.01$). Error bars represent means ± SE (Stand Error) (n = 3). Three
893 independent experiments were carried out with similar results.
894

895 E. RT-PCR analysis of the expression of *NRG1C* and *DAR5* after *P.s.m.* ES4326
896 infection. Samples were collected at 0, 12 and 24 h after infection. Values were
897 normalized to the level of *ACTIN7* and the transcript levels at 0 h post-inoculation (hpi)
898 were set at 1.0. Error bars represent means ± SE (n = 3). Three independent experiments
899 were carried out with similar results.
900

901 **Figure 2. *NRG1C* negatively regulates *chs3-2D* and *snc1*-mediated autoimmunity.**
902

903 A. Morphology of four-week-old soil-grown plants of Col-0, *chs3-2D*, two independent
904 transgenic lines of *NRG1C OE* into *chs3-2D* background and *chs3-2D nrg1a nrg1b*. *OE*
905 stands for overexpression of *NRG1C*. Bar = 1cm.
906

907 B. *NRG1C* gene expression in the indicated genotypes as determined by RT-PCR (*chs3-*
908 *2D* serves as control whose *NRG1C* transcript level was set at 1.0). Statistical
909 significance is indicated by different letters ($p < 0.01$). Error bars represent means ± SE
910 (n = 3). Two independent experiments were carried out with similar results.
911

912 C. Fresh weights of plants in (A). Statistical significance is indicated by different letters
913 ($p < 0.01$). Error bars represent means ± SE (n=7).
914

915 D. Quantification of *H.a.* Noco2 sporulation in the indicated genotypes 7 days post
916 inoculation (dpi) with 10^5 spores per ml water. Statistical significance is indicated by
917 different letters ($p < 0.01$). Error bars represent means ± SE (n=4). Three independent
918 experiments were carried out with similar results.
919

920 E. *NRG1C* gene expression in the indicated plants as determined by RT-PCR (*snc1* serves
921 as control whose *NRG1C* transcript level was set at 1.0). Statistical significance is
922 indicated by different letters ($p < 0.01$). Error bars represent means ± SE (n = 3). Two
923 independent experiments were carried out with similar results.
924

925 F. Morphology of four-week-old soil-grown plants of Col-0, *snc1*, two independent
926 transgenic lines of *NRG1C OE* into *snc1* background and *snc1 nrg triple*. Bar = 1cm.
927
928 G. Fresh weights of plants in (F). Statistical significance is indicated by different letters
929 ($p < 0.01$). Error bars represent means ± SE (n=7). The color legends are included in I.
930
931 H. Quantification of *H.a.* Noco2 sporulation in the indicated genotypes at 7 dpi with 10^5
932 spores per ml water. Statistical significance is indicated by different letters ($p < 0.01$).
933 Error bars represent means ± SE (n=4). Three independent experiments were carried out
934 with similar results. The color legends are included in I.
935
936 I. Bacterial growth of *P.s.t.* DC3000 in four-week-old leaves of the indicated genotypes
937 at 0 and 3 dpi with bacterial inoculum of OD_{600} = 0.001. Statistical significance is
938 indicated by different letters ($p < 0.01$). Error bars represent means ± SE (n=4). Three
939 independent experiments were carried out with similar results.
940
941 **Figure 3. NRG1C antagonizes HopQ1-1-mediated defense and AvrRPS4-mediated**
942 **HR.**
943

944 A. Growth of *P.s.t.* CUCPB5500 and *P.s.t.* CUCPB5500 HopQ1-1 in four-week-old
945 leaves of the indicated genotypes at 0 and 3 dpi with bacterial inoculum of OD_{600} =
946 0.0005. Statistical significance is indicated by different letters ($p < 0.01$). Error bars
947 represent means ± SE (n=4). Three independent experiments were carried out with
948 similar results.
949
950 B. HR observation of leaves infiltrated with *Pf0-1*_AvrRPS4. Four-week-old *A. thaliana*
951 leaves of the indicated genotypes were infiltrated with *Pf0-1* expressing AvrRPS4 at
952 OD_{600} = 0.2. Photographs were taken at 36 hpi. The numbers indicate the number of
953 plants displaying HR out of the total number of plants tested. Three independent
954 experiments were carried out with similar results.
955
956 C. Ion leakage of *A. thaliana* leaves upon *Pf0-1*_AvrRPS4 infiltration under the same
957 conditions as for B. Each dot represents four technical replicates from one independent
958 experiment. Statistical significance is indicated by different letters ($p < 0.01$). Error bars
959 represent means ± SE (n=3). Three independent experiments were carried out with
960 similar results.
961
962 **Figure 4. NRG1C works along the EDS1-NRG1-SAG101 module, in parallel with**
963 **the EDS1-ADR1-PAD4 module.**
964

965 A. Morphology of four-week-old soil-grown plants of Col-0, *snc1*, *snc1 eds1*-2, *snc1*
966 *pad4-1*, *snc1 adr1 triple*, *snc1 sag101-1*, *snc1 nrg triple*, *snc1 pad4-c1 adr1 triple*, *snc1*
967 *sag101-1 nrg triple*, *snc1 pad4-c1 sag101-1*, *snc1 pad4-c1 nrg triple*, *snc1 sag101-c1*
968 *adr1 triple* and *snc1 adr1 triple nrg triple*. *pad4-c1* and *sag101-c1* alleles were generated
969 through the CRISPR-Cas9 system. Bar = 1cm.

970
971 B. *PR1* gene expression in the indicated genotypes as determined by RT-PCR (Col-0
972 serves as control whose *PR1* transcript level was set at 1.0). Statistical significance is
973 indicated by different letters ($p < 0.01$). Error bars represent means ± SE (n = 3). Two
974 independent experiments were carried out with similar results.
975

976 C. Morphology of four-week-old soil-grown plants of Col-0, *snc1*, *snc1 nrg triple*, *snc1*
977 *sag101-1*, *snc1 NRG1C* OE, *snc1 nrg triple NRG1C OE* and *snc1 sag101-1 NRG1C OE*.
978 *OE* stands for overexpression of *NRG1C*. Bar = 1cm.
979
980 **Figure 5. NRG1C regulates *chs3-2D*-mediated autoimmunity through processes**
981 **unrelated to transcriptional interference.**
982

983 A. Morphology of four-week-old soil-grown plants of Col-0, *chs3-2D*, and two
984 independent transgenic lines of $NRG1C^{T71*}$ *OE* into *chs3-2D* background. *OE* stands for
985 overexpression of $NRG1C^{T71*}$, which carries an early stop codon to disrupt protein
986 synthesis, but not transcription. Bar = 1cm.
987
988 B. $NRG1C^{T71*}$ gene expression in the indicated genotypes as determined by RT-PCR
989 (*chs3-2D* serves as control whose *NRG1C* transcript level was set at 1.0). Statistical
990 significance is indicated by different letters ($p < 0.01$). Error bars represent means ± SE
991 (n = 3). Two independent experiments were carried out with similar results.
992
993 C. Fresh weights of plants in (A). Statistical significance is indicated by different letters
994 ($p < 0.01$). Error bars represent means ± SE (n=7).
995
996 D. Quantification of *H.a.* Noco2 sporulation in the indicated genotypes at 7 dpi with 10^5
997 spores per ml water. Statistical significance is indicated by different letters ($p < 0.01$).
998 Error bars represent means ± SE (n=4). Three independent experiments were carried out
999 with similar results.
1000
1001 **Figure 6. NRG1C antagonizes NRG1A *D485V*-mediated autoimmunity through**
1002 **associating with EDS1-SAG101 complex.**
1003

1004 A. Morphology of three-week-old soil-grown plants of Col-0, *NRG1A D485V*, and three
1005 independent transgenic lines of *NRG1C OE* into *NRG1A D485V* background. *OE* stands
1006 for overexpression of *NRG1C*. *NRG1A D485V* was tagged with three FLAG epitopes in
1007 frame at its C-terminus. Bar = 1cm.
1008
1009 B. Quantification of *H.a.* Noco2 sporulation in the indicated genotypes at 7 dpi with 10^5
1010 spores per ml water. Statistical significance is indicated by different letters ($p < 0.01$).
1011 Error bars represent means ± SE (n=4). Three independent experiments were carried out
1012 with similar results.
1013

1014 C. Immunoblot analysis of NRG1A D485V protein levels in the indicated genotypes.
1015 Equal loading is shown by Ponceau S staining of a non-specific band. The numbers
1016 below represent the normalized ratio between the intensity of the protein band and the
1017 Ponceau S band ± SE (n=3). Molecular mass marker in kiloDaltons is indicated on the
1018 left.
1019
1020 D. Immunoprecipitation and biotinylation of NRG1C-3FLAG and SAG101-3FLAG by
1021 EDS1-HA-TurboID in *N. benthamiana* in the presence of RBA1. Immunoprecipitation
1022 was carried out with anti-FLAG beads. The 3FLAG-tagged proteins were detected using
1023 an anti-FLAG antibody. The HA-TurboID-tagged proteins were detected using an anti-
1024 HA antibody. The biotinylated proteins were detected using Streptavidin-HRP. Molecular
1025 mass marker in kiloDaltons is indicated on the left. The experiment was repeated three
1026 times with similar results.

1027
1028 E. Biotinylation of SAG101-3FLAG by NRG1C-HA-TurboID in *A. thaliana* plants
1029 stably transformed with the two transgenes in the presence of RBA1.
1030 Immunoprecipitation was carried out with anti-FLAG beads. The 3FLAG-tagged proteins
1031 were detected using an anti-FLAG antibody. The HA-TurboID-tagged proteins were
1032 detected using an anti-HA antibody. EDS1 was detected using an anti-EDS1 antibody.
1033 The biotinylated proteins were detected using HRP-Streptavidin. Molecular mass marker
1034 in kiloDaltons is indicated on the left. The experiment was repeated twice with similar
1035 results.

1036 **Figure 7. NRG1C-type N-terminally truncated hNLR from canola (*Brassica napus***
1037 **L. cv. Westar) functions similarly as *A. thaliana* NRG1C.**
1038

1039 A. Morphology of four-week-old soil-grown plants of Col-0, *chs3-2D*, and two
1040 independent transgenic lines of *BraNRG1C OE* into *chs3-2D* background. Bar = 1cm.
1041
1042 B. *BraNRG1C* gene expression in the indicated plants as determined by RT-PCR.
1043 Statistical significance is indicated by different letters ($p < 0.01$). Error bars represent
1044 means ± SE (n = 3). ND stands for Not Detectable. Two independent experiments were
1045 carried out with similar results. The color legends are included in D.
1046
1047 C. Fresh weights of plants in (A). Statistical significance is indicated by different letters
1048 ($p < 0.01$). Error bars represent means ± SE (n=7). The color legends are included in D.
1049
1050 D. Quantification of *H.a.* Noco2 sporulation in the indicated genotypes at 7 dpi with 10^5
1051 spores per ml water. Statistical significance is indicated by different letters ($p < 0.01$).
1052 Error bars represent means ± SE (n=4). Three independent experiments were carried out
1053 with similar results.
1054

1055 E-F. HR observation of *N. benthamiana* leaves expressing the indicated proteins at 48 hpi
1056 following the infiltration of *P.s.t.* CUCPB5500 HopQ1-1 to deliver HopQ1-1 effector.
1057 Photographs were taken at 4 dpi after *P.s.t.* CUCPB5500 HopQ1-1 infiltration.
1058
1059 G-H. Ion leakage of *N. benthamiana* leaves upon *P.s.t.* CUCPB5500 HopQ1-1 infiltration
1060 under the same conditions as with E and F. Statistical significance is indicated by
1061 different letters ($p < 0.01$). Error bars represent means ± SE (n = 6). Three independent
1062 experiments were carried out with similar results.
1063
1064 I. A model of two defense modules downstream of TNL activation in Arabidopsis. An
1065 effector-induced TNL resistosome with NADase activity (Horsefield et al., 2019; Ma et
1066 al., 2020; Martin et al., 2020; Tian and Li, 2020; Wan et al., 2019) signals through two
1067 parallel modules, EDS1-PAD4-ADR1s and EDS1-SAG101-NRG1A/1B to activate
1068 defense responses. N-terminally truncated hNLR NRG1C antagonizes immunity
1069 mediated by its full-length neighbors NRG1A and NRG1B to avoid aberrant activation.
1070
1071
1072
1073 **Figure S1. Full-length protein sequence alignment of NRG1C and its orthologs in**
1074 **different plant species.**
1075
1076 Putative NRG1C orthologs were obtained from Phytozome (Brassicaceae species) and
1077 Sol Genomics Network (*N. benthamiana*) using *A. thaliana* NRG1C protein sequence as
1078 input. NB domain and LRR domain are indicated by single underline and double
1079 underline, respectively. P-loop motif is boxed in a black line.
1080

1081 **Figure S2. DAR5 has no effect on *chs3-2D* and *snc1*-mediated autoimmunity.**
1082

1083 A. Morphology of four-week-old soil-grown plants of Col-0, *chs3-2D*, and two
1084 independent transgenic lines of *DAR5 OE* into *chs3-2D* background. *OE* stands for
1085 overexpression of *DAR5*. Bar = 1cm.
1086
1087 B. *DAR5* gene expression in the indicated plants as determined by RT-PCR (*chs3-2D*
1088 serves as control whose *DAR5* transcript level was set at 1.0). Statistical significance is
1089 indicated by different letters ($p < 0.01$). Error bars represent means ± SE (n = 3). Two
1090 independent experiments were carried out with similar results.
1091
1092 C. Morphology of four-week-old soil-grown plants of Col-0, *snc1*, and two independent
1093 transgenic lines of *DAR5 OE* into *snc1* background. *OE* stands for overexpression of
1094 *DAR5*. Bar = 1cm.
1095
1096 D. *DAR5* gene expression in the indicated plants as determined by RT-PCR (*snc1* serves
1097 as control whose *DAR5* transcript level was set at 1.0). Statistical significance is indicated
1098 by different letters ($p < 0.01$). Error bars represent means ± SE (n = 3). Two independent
1099 experiments were carried out with similar results.

1100

1101 **Figure S3. Full-length protein sequence alignment of ADR1-L3 and its**
1102 **orthologs in different plant species.**
1103

1104 Putative ADR1-L3 orthologs were obtained from Phytozome using *A. thaliana* ADR1-L3
1105 protein sequence as input. RPW8 domain, NB domain and LRR domain are indicated by
1106 single underline, double underline and dashed underline, respectively.
1107
1108

1109 **Figure S4. No immune-related phenotypes were observed in *ADR1-L3***
1110 **overexpression lines.**
1111

1112 A. Morphology of four-week-old soil-grown plants of Col-0, *snc1*, and two independent
1113 transgenic lines of *ADR1-L3 OE* into *snc1* background. *OE* stands for overexpression of
1114 *ADR1-L3*. Bar = 1cm.
1115

1116 B. Quantification of *H.a.* Noco2 sporulation in the indicated genotypes at 7 dpi with 10^5
1117 spores per ml water. Statistical significance is indicated by different letters ($p < 0.01$).
1118 Error bars represent means ± SE (n=4). Three independent experiments were carried out
1119 with similar results.
1120

1121 C. Quantification of *H.a.* Emwa1 sporulation in the indicated genotypes at 7 dpi with 10^5
1122 spores per ml water. Statistical significance is indicated by different letters ($p < 0.01$).
1123 Error bars represent means ± SE (n=4). Three independent experiments were carried out
1124 with similar results.
1125
1126

1127 **Figure S5. Overexpression of *NRG1C* has no effect on *chs1-2* or *chs2-1*-mediated**
1128 **autoimmunity.**
1129

1130 A-B. Morphology of four-week-old soil-grown plants of Col-0, *chs1-2* (A), *chs2-1* (B)
1131 and two independent transgenic lines of *NRG1C OE* into *chs1-2* (A) and *chs2-1* (B)
1132 backgrounds. Plants were grown at 16 °C under long day conditions. Bar = 1cm.
1133

1134 C. Morphology of four-week-old soil-grown plants of Col-0 and two independent
1135 transgenic lines of *NRG1C OE* in Col-0 background. Bar = 1cm.
1136

1137 D. Quantification of *H.a.* Emwa1 sporulation in the indicated genotypes at 7 dpi with 10^5
1138 spores per ml water. Statistical significance is indicated by different letters ($p < 0.01$).
1139 Error bars represent means ± SE (n=4). Three independent experiments were carried out
1140 with similar results.
1141

1142 **Figure S6. NRG1C does not affect TNL RPS4 or CNL RPS2-mediated bacterial**
1143 **growth and basal defense.**
1144

1145 A-C. Growth of *P.s.t. avrRps4* (A), *avrRpt2* (B) and *P.s.t.* DC3000 (C) in four-week-old
1146 leaves of the indicated genotypes at 0 dpi and 3 dpi with bacterial inoculum of OD_{600} =
1147 0.001. Statistical significance is indicated by different letters ($p < 0.01$). Error bars
1148 represent means ± SE (n=4). Three independent experiments were carried out with
1149 similar results.
1150

1151 **Figure S7. Schematic description of CRISPR/Cas9 construct design to delete *PAD4***
1152 **or *SAG101*.**
1153

1154 Red arrows indicate the location of two guide RNA target sites. Target sequences are
1155 shown in the below. The letters in red indicate the NGG PAM sequences. Scissors
1156 indicate where the Cas9 cut the genomic sequence.
1157
1158 **Figure S8. NRG1C works in the same pathway with the EDS1-NRG1-SAG101**
1159 **module.**
1160

1161 A-B. *PR1* gene expression in the indicated genotypes as determined by RT-PCR (Col-0
1162 serves as control whose *PR1* transcript level was set at 1.0). Statistical significance is
1163 indicated by different letters ($p < 0.01$). Error bars represent means ± SE (n = 3). Two
1164 independent experiments were carried out with similar results.
1165

1166
1167 **Figure S9. NRG1C antagonizes NRG1A D485V-mediated HR.**
1168
1169 A. *NRG1C* gene expression in the indicated plants as determined by RT-PCR (*NRG1A*
1170 *D485V* serves as control whose *NRG1C* transcript level was set at 1.0). Statistical
1171 significance is indicated by different letters ($p < 0.01$). Error bars represent means ± SE
1172 (n = 3). Two independent experiments were carried out with similar results.
1173
1174 B. HR in the *N. benthamiana* leaves expressing NRG1A D485V-3FLAG and EV (Empty
1175 Vector) in the absence (right) or presence (left) of NRG1C. Photos were taken at 4 dpi.
1176 Three independent experiments were carried out with similar results.
1177
1178 C. Ion leakage of *N. benthamiana* leaves upon *Agrobacterium* infiltration under the same
1179 conditions as for B. Statistical significance is indicated by different letters ($p < 0.01$).
1180 Error bars represent means ± SE (n = 3). Three independent experiments were carried out
1181 with similar results.
1182
1183 D. Immunoblot analysis of protein levels of NRG1A D485V-3FLAG in leaves of B.
1184 Samples were harvest at 24 hpi, when no macroscopic HR was visible. Equal loading is

shown by Ponceau S staining of a non-specific band. The numbers below represent the normalized ratio between the intensity of the protein band and the Ponceau S band ± SE (n=3). Molecular mass marker in kiloDaltons is indicated on the left.

Figure S10. NRG1C does not influence the autoimmunity of *ADR1-L2 D484V*.

A. Morphology of three-week-old soil-grown plants of Col-0, *ADR1-L2 D484V*, and two independent transgenic lines of *NRG1C OE* into *ADR1-L2 D484V* background. *OE* stands for overexpression of *NRG1C*. Bar = 1cm.

B. Fresh weights of plants in (A). Statistical significance is indicated by different letters ($p < 0.01$). Error bars represent means ± SE (n=7).

C. Quantification of *H.a.* Noco2 sporulation in the indicated genotypes at 7 dpi with 10^5 spores per ml water. Statistical significance is indicated by different letters ($p < 0.01$). Error bars represent means ± SE (n=4). Three independent experiments were carried out with similar results.

Figure S11. NRG1C does not associate with full-length NRG1A.

A. HR in the WT or *nrg1-1 N. benthamiana* leaves expressing RBA1. Photos were taken at 2 dpi. Three independent experiments were carried out with similar results.

B. Immunoprecipitation of NRG1C-3FLAG and biotinylation of NRG1C-3FLAG by NRG1A-HATurboID in *N. benthamiana* in the presence of RBA1. Immunoprecipitation was carried out with anti-FLAG beads. The 3FLAG-tagged proteins were detected using an anti-FLAG antibody. The HA-TurboID-tagged proteins were detected using an anti-HA antibody. The biotinylated proteins were detected using Streptavidin-HRP. Molecular mass marker in kiloDaltons is indicated on the left. Three independent experiments were carried out with similar results.

Figure S12. The association between NRG1C with EDS1-SAG101 complex depends on TIR induction and SAG101.

A. Immunoprecipitation and biotinylation of NRG1C-3FLAG and SAG101-3FLAG by EDS1-HA-TurboID in *N. benthamiana* in the absence of RBA1. Immunoprecipitation was carried out with anti-FLAG beads. The 3FLAG-tagged proteins were detected using an anti-FLAG antibody. The HA-TurboID-tagged proteins were detected using an anti-HA antibody. The biotinylated proteins were detected using Streptavidin-HRP. Molecular mass marker in kiloDaltons is indicated on the left. Three independent experiments were carried out with similar results.

1228 B. Immunoprecipitation and biotinylation of NRG1C-3FLAG or/and SAG101-3FLAG
1229 by EDS1-HA-TurboID in *N. benthamiana*. Immunoprecipitation was carried out with
1230 anti-FLAG beads. The 3FLAG-tagged proteins were detected using an anti-FLAG
1231 antibody. The HA-TurboID-tagged proteins were detected using an anti-HA antibody.
1232 The biotinylated proteins were detected using Streptavidin-HRP. Molecular mass marker
1233 in kiloDaltons is indicated on the left. Three independent experiments were carried out
1234 with similar results.
1235

1236 **Figure S13. Overexpression of *NRG1C* does not affect the protein levels of EDS1 and**
1237 **SAG101.**
1238

1239 A. Immunoblot analysis of protein levels of EDS1-ZZ-TEV-FLAG in the absence or
1240 presence of NRG1C-3FLAG. Equal loading is shown by Ponceau S staining of a non-
1241 specific band. Molecular mass marker in kiloDaltons is indicated on the left.
1242
1243 B. Quantification of band intensity of (A). The numbers represent the normalized ratio
1244 between the intensity of the protein band and the Ponceau S band ± SE (n=8).
1245
1246 C. Immunoblot analysis of protein levels of SAG101-3FLAG in the absence or presence
1247 of NRG1C-3FLAG. Equal loading is shown by Ponceau S staining of a non-specific
1248 band. Molecular mass marker in kiloDaltons is indicated on the left.
1249
1250 D. Quantification of band intensity of C. The numbers represent the normalized ratio
1251 between the intensity of the protein band and the Ponceau S band ± SE (n=8).
1252

1253 **Figure S14. TIR NADase enzyme activity promotes the association between NRG1C**
1254 **with EDS1-SAG101 complex, and NRG1C does not associate with the EDS1-PAD4**
1255 **complex.**
1256

1257 A. Immunoprecipitation and biotinylation of NRG1C-3FLAG and SAG101-3FLAG by
1258 EDS1-HA-TurboID in *N. benthamiana* in the presence of $RBA1_{E86A}$.
1259 Immunoprecipitation was carried out with anti-FLAG beads. The 3FLAG-tagged proteins
1260 were detected using an anti-FLAG antibody. The HA-TurboID-tagged proteins were
1261 detected using an anti-HA antibody. The biotinylated proteins were detected using
1262 Streptavidin-HRP. Molecular mass marker in kiloDaltons is indicated on the left. Three
1263 independent experiments were carried out with similar results.
1264
1265 B. Immunoprecipitation and biotinylation of NRG1C-3FLAG and PAD4-ZZ-TEV-FLAG
1266 by EDS1-HA-TurboID in *N. benthamiana* in the presence of RBA1. Immunoprecipitation
1267 was carried out with anti-FLAG beads. The ZZ-TEV-FLAG and 3FLAG-tagged proteins
1268 were detected using an anti-FLAG antibody. The HA-TurboID-tagged proteins were
1269 detected using an anti-HA antibody. The biotinylated proteins were detected using
1270 Streptavidin-HRP. Molecular mass marker in kiloDaltons is indicated on the left. Three
1271 independent experiments were carried out with similar results.

1272

1273 **C. The normalized ratio between the intensity of the NRG1C band and the SAG101**
1274 **band in different treatments. As EDS1 constitutively associates with SAG101,**
1275 **SAG101 bands were used as controls.**

1276

1277 **Figure S15. Brassicaceae NRG1C ortholog does not influence HopQ1-1-mediated**
1278 **HR in *N. benthamiana*.**
1279

1280 A. Schematic showing *N. benthamiana* transient expression assays to test protein
1281 functionalities in HopQ1-1-dependent HR by infiltrating with *P.s.t.* CUCPB5500 HopQ1-
1282 1 (see Methods for details).
1283
1284 B-C. *NbNRG2* (B) and *NRG1C* (C) genes expression in the indicated leaves as
1285 determined by RT-PCR. Statistical significance is indicated by different letters ($p < 0.01$).
1286 Error bars represent means ± SE (n = 3). The *NbNRG2* transcript level in the presence of
1287 EV treatment was set at 1.0. Two independent experiments were carried out with similar
1288 results.
1289
1290 D. HR in the *N. benthamiana* leaves expressing the indicated proteins at 48 hpi following
1291 the infiltration of *P.s.t.* CUCPB5500 HopQ1-1 to deliver HopQ1-1 effector. Photographs
1292 were taken at 4 dpi after *P.s.t.* CUCPB5500 HopQ1-1 infiltration.
1293
1294 E. Ion leakage of *N. benthamiana* leaves upon *P.s.t.* CUCPB5500 HopQ1-1 infiltration in
1295 the same conditions as for the photographs in D. Statistical significance is indicated by
1296 different letters ($p < 0.01$). Error bars represent means ± SE (n = 6). Three independent
1297 experiments were carried out with similar results.
1298
1299 F. *BraNRG1C* gene expression in the indicated leaves as determined by RT-PCR. Error
1300 bars represent means ± SE (n = 3). Two independent experiments were carried out with
1301 similar results.
1302
1303
1304 **Figure S16. NbNRG2 does not influence *chs3-2D*-mediated autoimmunity.**

1305 A. Morphology of four-week-old soil-grown plants of Col-0, *chs3-2D*, and two
1306 independent transgenic lines of *NbNRG2 OE* into *chs3-2D* background. *OE* stands for
1307 overexpression of *NbNRG2*. Bar = 1cm.

1308

1309 B. *NbNRG2* expression level in the indicated plants as determined by RT-PCR. Statistical
1310 significance is indicated by different letters ($p < 0.05$). Error bars represent means ± SE
1311 (n = 3). Three independent experiments were carried out with similar results.
1312
1313 C. Fresh weights of plants in (A). Statistical significance is indicated by different letters
1314 ($p < 0.01$). Error bars represent means ± SE (n=6).

1315
1316 D. Quantification of *H.a.* Noco2 sporulation in the indicated genotypes at 7 dpi with 10^5
1317 spores per ml water. Statistical significance is indicated by different letters ($p < 0.01$).
1318 Error bars represent means ± SE (n=4). Three independent experiments were carried out
1319 with similar results.
1320

1321 **Table S1. The genome arrangement of NRG1C in plant species.**

1322 Arrows in tandem indicate tandemly arranged genes, while arrows in rows indicate
1323 randomly assorted genes on different scaffolds. All sequences were obtained from
1324 Phytozome. *A. thaliana* (*AT5G66910*, *AT5G66900*, *AT5G66890*); *Arabidopsis lyrate*
1325 (*AL8G44490*, *AL8G44500*, *AL8G44510*); *Arabidopsis haller* (*Araha.11408s0003.1*,
1326 *Araha.11408s0002.1*); *Boechera stricta* (*Bostr.27102s0001.1*; *Bostr.0568s0113.1*);
1327 *Capsella grandiflora* (*Cagra.2007s0011.1*, *Cagra.2007s0012.1*); *Capsella rubella*
1328 (*Carubv 10027991m*, *Carubv10028036m*); *Eutrema salsugineum* (*Thhalv10003662m*,
1329 *Thhalv10005443m*, *Thhalv10005517m*; *Thhalv10020099m*); *Brassica rapa*
1330 (*Brara.I00877.1*, *Brara.I00876.1*; *Brara.G01212.1*, *Brara.G01211.1*; *Brara.B03562.1*;
1331 *Brara.F02778.1*). All truncated NRG1C orthologs are labeled with yellow arrows.
1332 Orange arrow indicates *Brara*.G01211.1.
1333

1334 **Table S2. The genome arrangement of *NL* truncated genes in *A. thaliana*.**

1335 Arrows in tandem indicate tandemly arranged genes. Dashed line indicates two genes are
1336 clustered, but not tandemly arranged. Gene codes are shown under the arrows. Orange,
1337 yellow, black, and blue arrows indicate CN, NL, full-length NLR, TIR-only proteins,
1338 respectively.

1339 **Table S3. The list of primers used in this study.**

1340

Figure 1

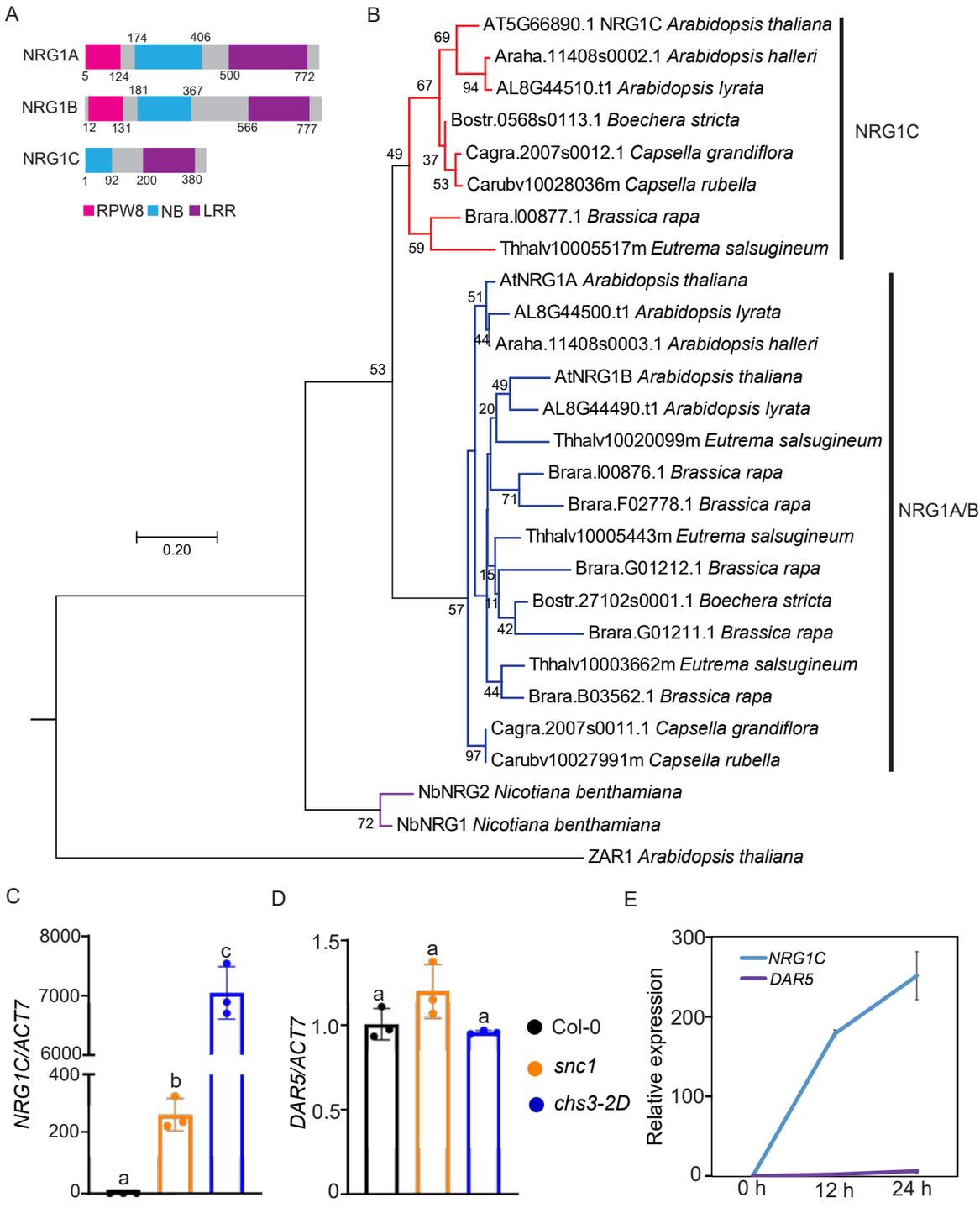

Figure 1. *NRG1C* is evolutionarily conserved in Brassicaceae, and its transcription is induced in TNL type autoimmune mutants and upon pathogen infection.

A. Protein domain diagram of NRG1A, NRG1B and NRG1C. Numbers represent amino acid positions relative to the translation start sites. NRG1C lacks the RPW8 CC and part of the NB domains.

B. Phylogenetic tree of putative NRG1A/1B/1C orthologs. Putative NRG1A/1B/1C orthologs were obtained from Phytozome (Brassicaceae species) and Sol Genomics Network (*N. benthamiana*) using *A. thaliana* NRG1A, NRG1B and NRG1C protein sequences as input, respectively. ZAR1 was used as an outgroup to root the tree. MUSCLE was used for sequence alignment and a Neighbor-joining tree was generated by using full-length NRG1C and homologous parts of all other corresponding NRG1 homologs with JTT model and using 2000 bootstrap replicates in MEGA 7.0.

C-D. *NRG1C* (C) and *DAR5* (D) gene expression in the autoimmune mutants *snc1* and *chs3-2D* as determined by RT-PCR (Col-0 serves as wild type control and the transcript level in Col-0 was arbitrarily set at 1.0). Statistical significance is indicated by different letters ($p < 0.01$). Error bars represent means ± SE (Stand Error) (n = 3). Three independent experiments were carried out with similar results.

E. RT-PCR analysis of the expression of *NRG1C* and *DAR5* after *P.s.m.* ES4326 infection. Samples were collected at 0, 12 and 24 h after infection. Values were normalized to the level of *ACTIN7* and the transcript levels at 0 h post-inoculation (hpi) were set at 1.0. Error bars represent means ± SE (n = 3). Three independent experiments were carried out with similar results.

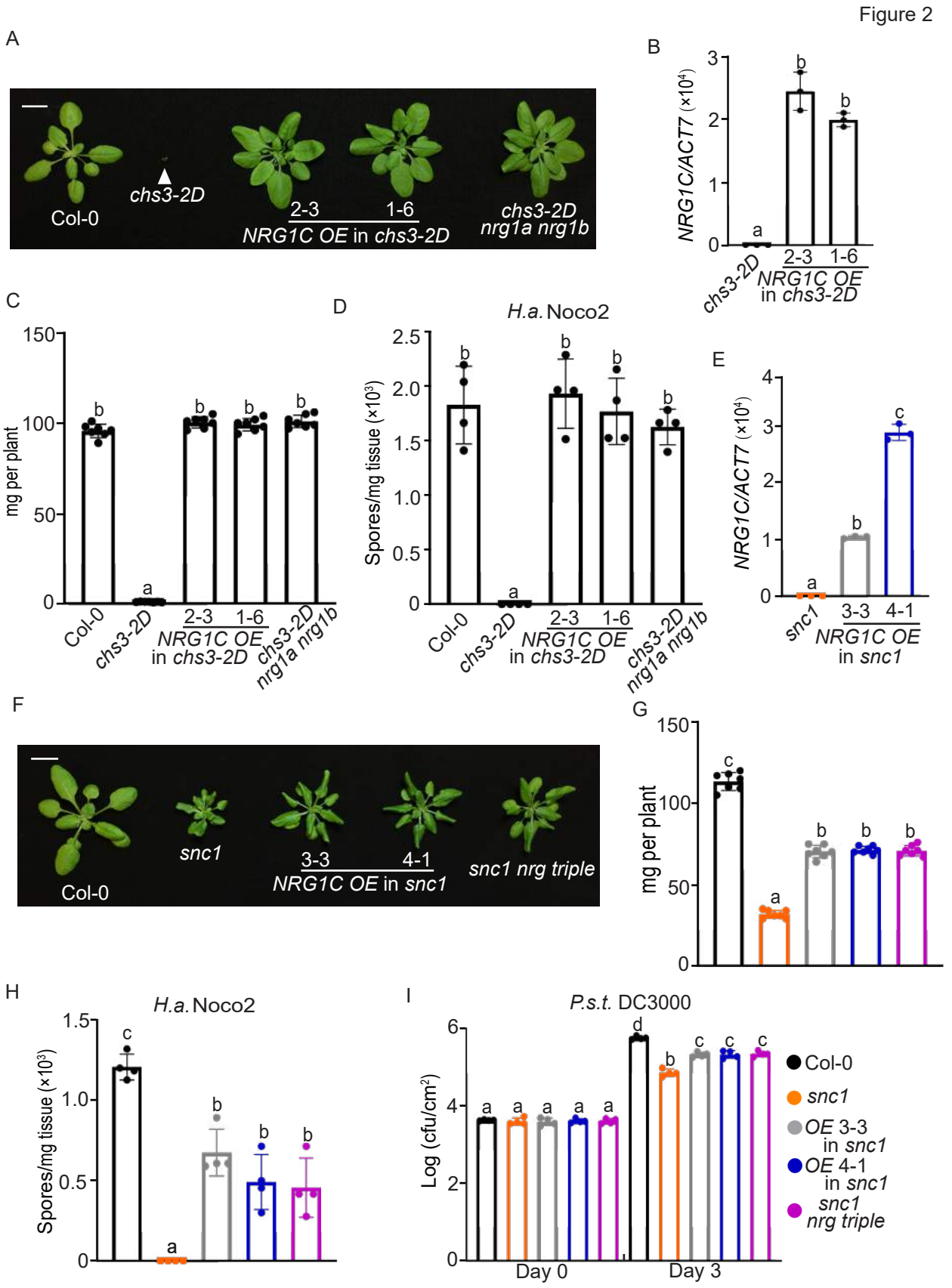

Figure 2. *NRG1C* negatively regulates *chs3-2D* and *snc1*-mediated autoimmunity.

A. Morphology of four-week-old soil-grown plants of Col-0, *chs3-2D*, two independent transgenic lines of *NRG1C OE* into *chs3-2D* background and *chs3-2D nrg1a nrg1b*. *OE* stands for overexpression of *NRG1C*. Bar = 1cm.

B. *NRG1C* gene expression in the indicated genotypes as determined by RT-PCR (*chs3-2D* serves as control whose *NRG1C* transcript level was set at 1.0). Statistical significance is indicated by different letters ($p < 0.01$). Error bars represent means ± SE (n = 3). Two independent experiments were carried out with similar results.

C. Fresh weights of plants in (A). Statistical significance is indicated by different letters ($p < 0.01$). Error bars represent means ± SE (n=7).

D. Quantification of *H.a.* Noco2 sporulation in the indicated genotypes 7 days post inoculation (dpi) with 10^5 spores per ml water. Statistical significance is indicated by different letters ($p < 0.01$). Error bars represent means ± SE (n=4). Three independent experiments were carried out with similar results.

E. *NRG1C* gene expression in the indicated plants as determined by RT-PCR (*snc1* serves as control whose *NRG1C* transcript level was set at 1.0). Statistical significance is indicated by different letters ($p < 0.01$). Error bars represent means ± SE (n = 3). Two independent experiments were carried out with similar results.

F. Morphology of four-week-old soil-grown plants of Col-0, *snc1*, two independent transgenic lines of *NRG1C OE* into *snc1* background and *snc1 nrg triple*. Bar = 1cm.

G. Fresh weights of plants in (F). Statistical significance is indicated by different letters ($p < 0.01$). Error bars represent means ± SE (n=7). The color legends are included in I.

H. Quantification of *H.a.* Noco2 sporulation in the indicated genotypes at 7 dpi with 10^5 spores per ml water. Statistical significance is indicated by different letters ($p < 0.01$). Error bars represent means ± SE (n=4). Three independent experiments were carried out with similar results. The color legends are included in I.

I. Bacterial growth of *P.s.t.* DC3000 in four-week-old leaves of the indicated genotypes at 0 and 3 dpi with bacterial inoculum of $OD_{600} = 0.001$. Statistical significance is indicated by different letters ($p < 0.01$). Error bars represent means ± SE (n=4). Three independent experiments were carried out with similar results.

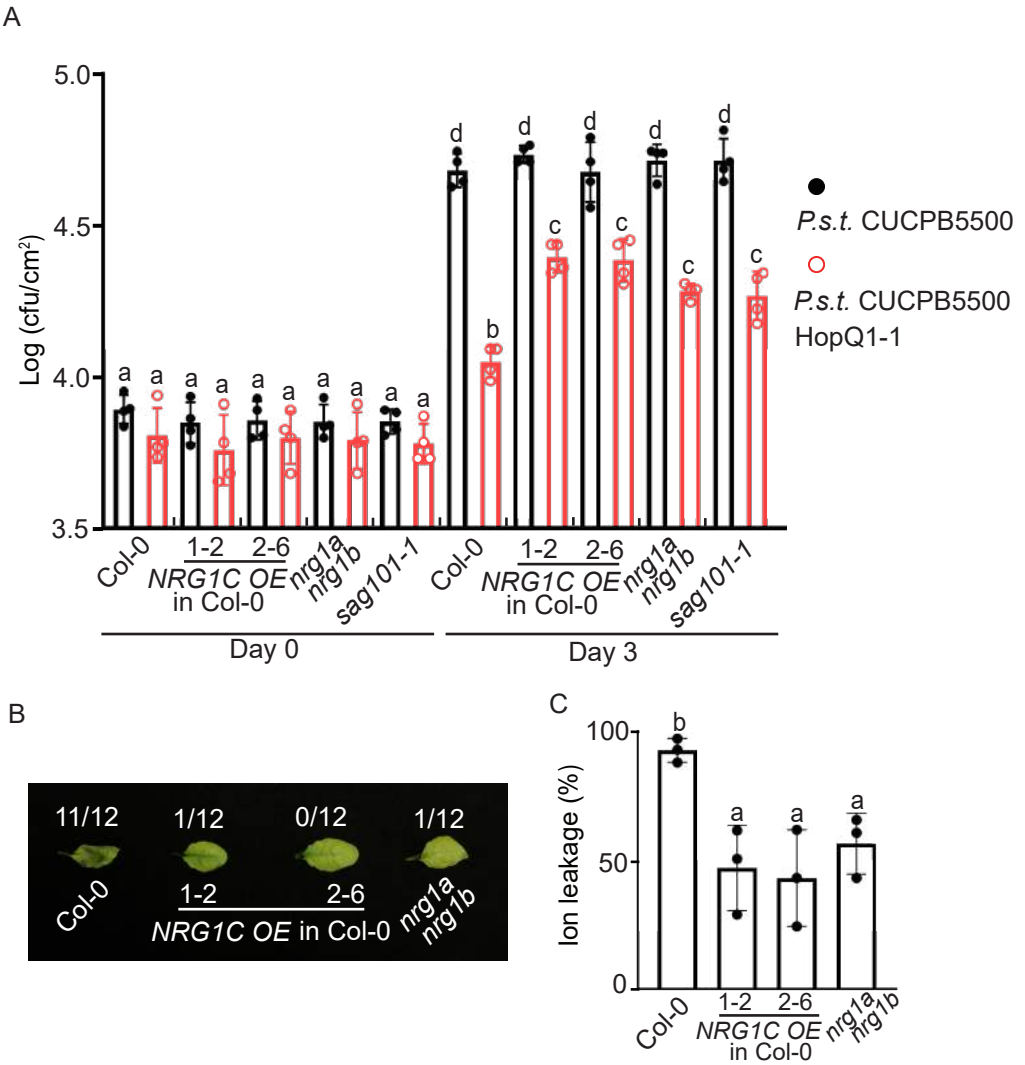

Figure 3. NRG1C antagonizes HopQ1-1-mediated defense and AvrRPS4-mediated HR.

A. Growth of *P.s.t.* CUCPB5500 and *P.s.t.* CUCPB5500 HopQ1-1 in four-week-old leaves of the indicated genotypes at 0 and 3 dpi with bacterial inoculum of OD_{600} = 0.0005. Statistical significance is indicated by different letters ($p < 0.01$). Error bars represent means ± SE (n=4). Three independent experiments were carried out with similar results.

B. HR observation of leaves infiltrated with *Pf0-1*_AvrRPS4. Four-week-old *A. thaliana* leaves of the indicated genotypes were infiltrated with *Pf0-1* expressing AvrRPS4 at OD_{600} = 0.2. Photographs were taken at 36 hpi. The numbers indicate the number of plants displaying HR out of the total number of plants tested. Three independent experiments were carried out with similar results.

C. Ion leakage of *A. thaliana* leaves upon *Pf0-1*_AvrRPS4 infiltration under the same conditions as for B. Each dot represents four technical replicates from one independent experiment. Statistical significance is indicated by different letters ($p < 0.01$). Error bars represent means ± SE (n=3). Three independent experiments were carried out with similar results.

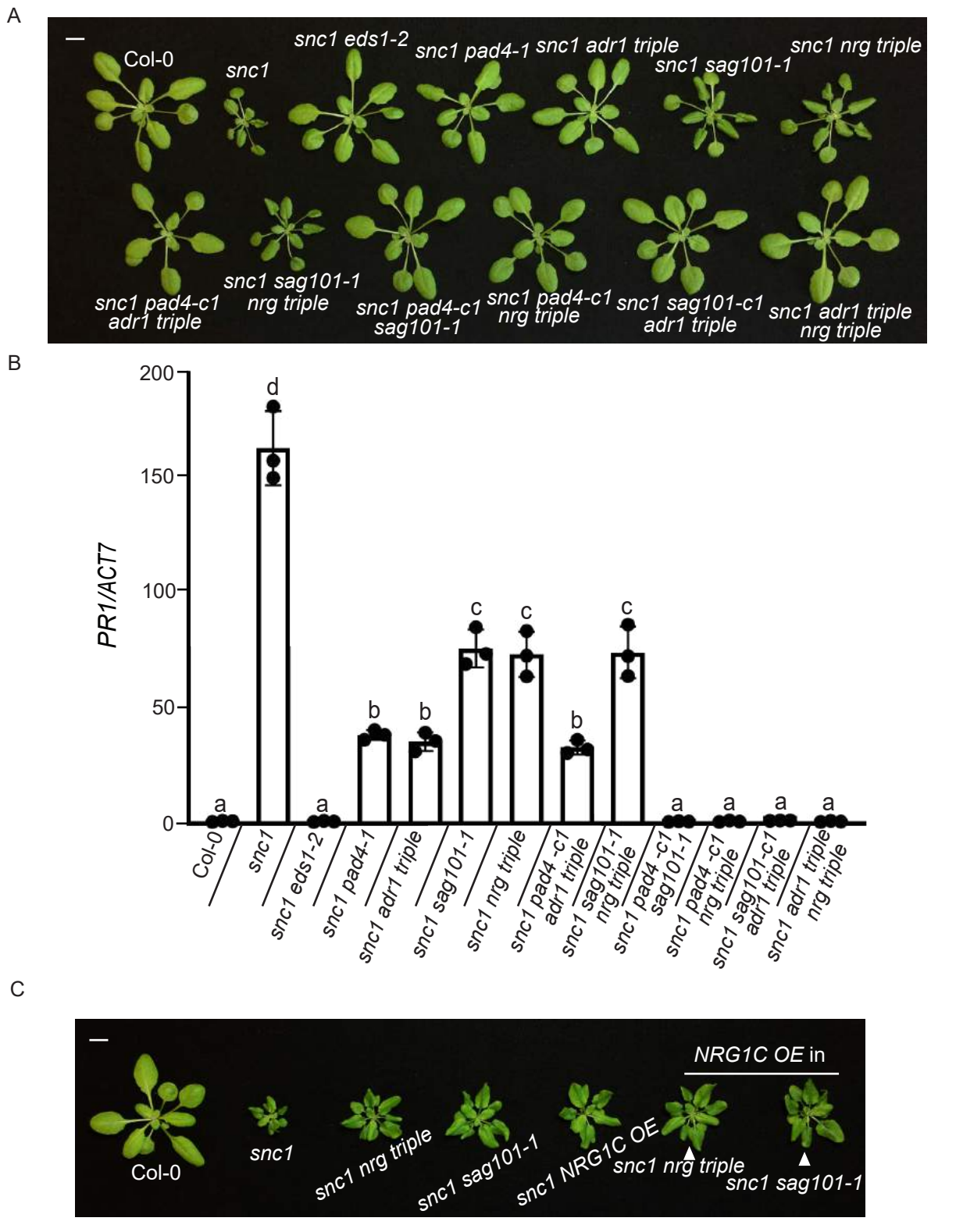

Figure 4. NRG1C works along the EDS1-NRG1-SAG101 module, in parallel with the EDS1-ADR1-PAD4 module.

A. Morphology of four-week-old soil-grown plants of Col-0, *snc1*, *snc1 eds1*-2, *snc1 pad4-1*, *snc1 adr1 triple*, *snc1 sag101-1*, *snc1 nrg triple*, *snc1 pad4-c1 adr1 triple*, *snc1 sag101-1 nrg triple*, *snc1 pad4-c1 sag101-1*, *snc1 pad4-c1 nrg triple*, *snc1 sag101-c1 adr1 triple* and *snc1 adr1 triple nrg triple*. *pad4-c1* and *sag101-c1* alleles were generated through the CRISPR-Cas9 system. Bar = 1cm.

B. *PR1* gene expression in the indicated genotypes as determined by RT-PCR (Col-0 serves as control whose *PR1* transcript level was set at 1.0). Statistical significance is indicated by different letters ($p < 0.01$). Error bars represent means ± SE (n = 3). Two independent experiments were carried out with similar results.

C. Morphology of four-week-old soil-grown plants of Col-0, *snc1*, *snc1 nrg triple*, *snc1 sag101-1*, *snc1 NRG1C* OE, *snc1 nrg triple NRG1C OE* and *snc1 sag101-1 NRG1C OE*. *OE* stands for overexpression of *NRG1C*. Bar = 1cm.

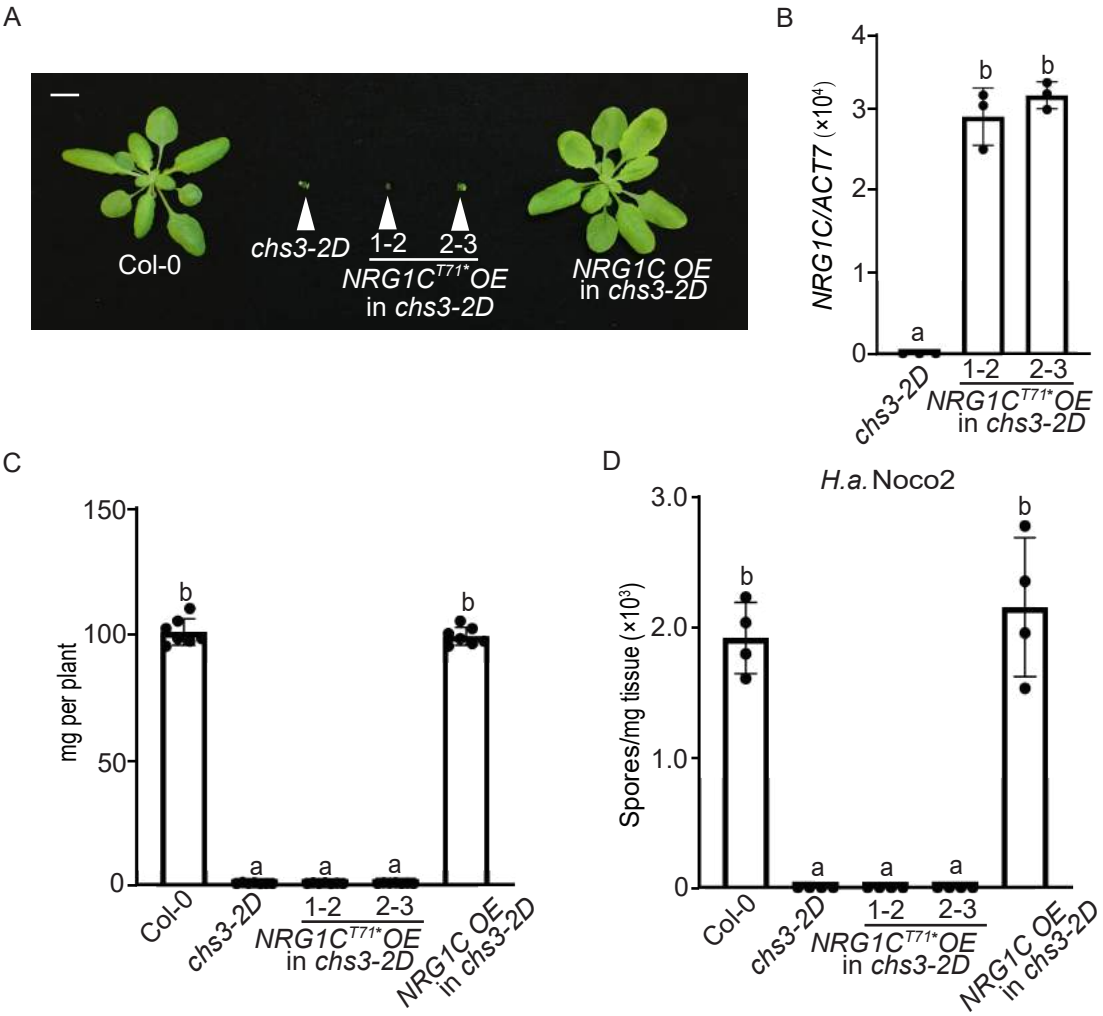

Figure 5. NRG1C regulates *chs3-2D*-mediated autoimmunity through processes unrelated to transcriptional interference.

A. Morphology of four-week-old soil-grown plants of Col-0, *chs3-2D*, and two independent transgenic lines of *NRG1C*^{T71*} *OE* into *chs3-2D* background. *OE* stands for overexpression of *NRG1C*^{T71*}, which carries an early stop codon to disrupt protein synthesis, but not transcription. Bar = 1cm.

B. *NRG1C*^{T71*} gene expression in the indicated genotypes as determined by RT-PCR (*chs3-2D* serves as control whose *NRG1C* transcript level was set at 1.0). Statistical significance is indicated by different letters ($p < 0.01$). Error bars represent means ± SE (n = 3). Two independent experiments were carried out with similar results.

C. Fresh weights of plants in (A). Statistical significance is indicated by different letters ($p < 0.01$). Error bars represent means ± SE (n=7).

D. Quantification of *H.a.* Noco2 sporulation in the indicated genotypes at 7 dpi with 10^5 spores per ml water. Statistical significance is indicated by different letters ($p < 0.01$). Error bars represent means ± SE (n=4). Three independent experiments were carried out with similar results.

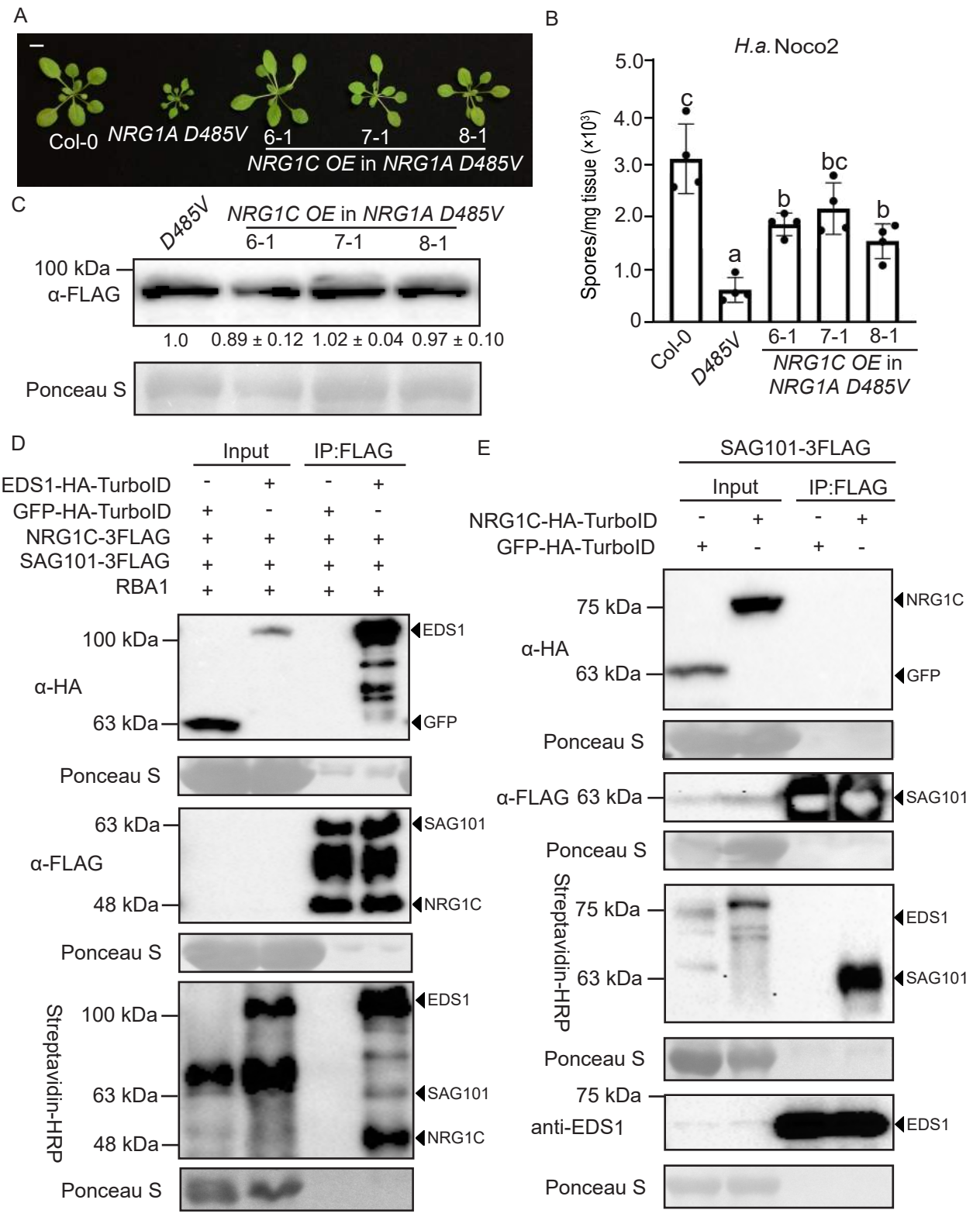

Figure 6. NRG1C antagonizes NRG1A *D485V*-mediated autoimmunity through associating with EDS1-SAG101 complex.

A. Morphology of three-week-old soil-grown plants of Col-0, *NRG1A D485V*, and three independent transgenic lines of *NRG1C OE* into *NRG1A D485V* background. *OE* stands for overexpression of *NRG1C*. *NRG1A D485V* was tagged with three FLAG epitopes in frame at its C-terminus. Bar = 1cm.

B. Quantification of *H.a.* Noco2 sporulation in the indicated genotypes at 7 dpi with 10^5 spores per ml water. Statistical significance is indicated by different letters ($p < 0.01$). Error bars represent means ± SE (n=4). Three independent experiments were carried out with similar results.

C. Immunoblot analysis of NRG1A D485V protein levels in the indicated genotypes. Equal loading is shown by Ponceau S staining of a non-specific band. The numbers below represent the normalized ratio between the intensity of the protein band and the Ponceau S band ± SE (n=3). Molecular mass marker in kiloDaltons is indicated on the left.

D. Immunoprecipitation and biotinylation of NRG1C-3FLAG and SAG101-3FLAG by EDS1-HA-TurboID in *N. benthamiana* in the presence of RBA1. Immunoprecipitation was carried out with anti-FLAG beads. The 3FLAG-tagged proteins were detected using an anti-FLAG antibody. The HA-TurboID-tagged proteins were detected using an anti-HA antibody. The biotinylated proteins were detected using Streptavidin-HRP. Molecular mass marker in kiloDaltons is indicated on the left. The experiment was repeated three times with similar results.

E. Biotinylation of SAG101-3FLAG by NRG1C-HA-TurboID in *A. thaliana* plants stably transformed with the two transgenes in the presence of RBA1. Immunoprecipitation was carried out with anti-FLAG beads. The 3FLAG-tagged proteins were detected using an anti-FLAG antibody. The HA-TurboID-tagged proteins were detected using an anti-HA antibody. EDS1 was detected using an anti-EDS1 antibody. The biotinylated proteins were detected using HRP-Streptavidin. Molecular mass marker in kiloDaltons is indicated on the left. The experiment was repeated twice with similar results.

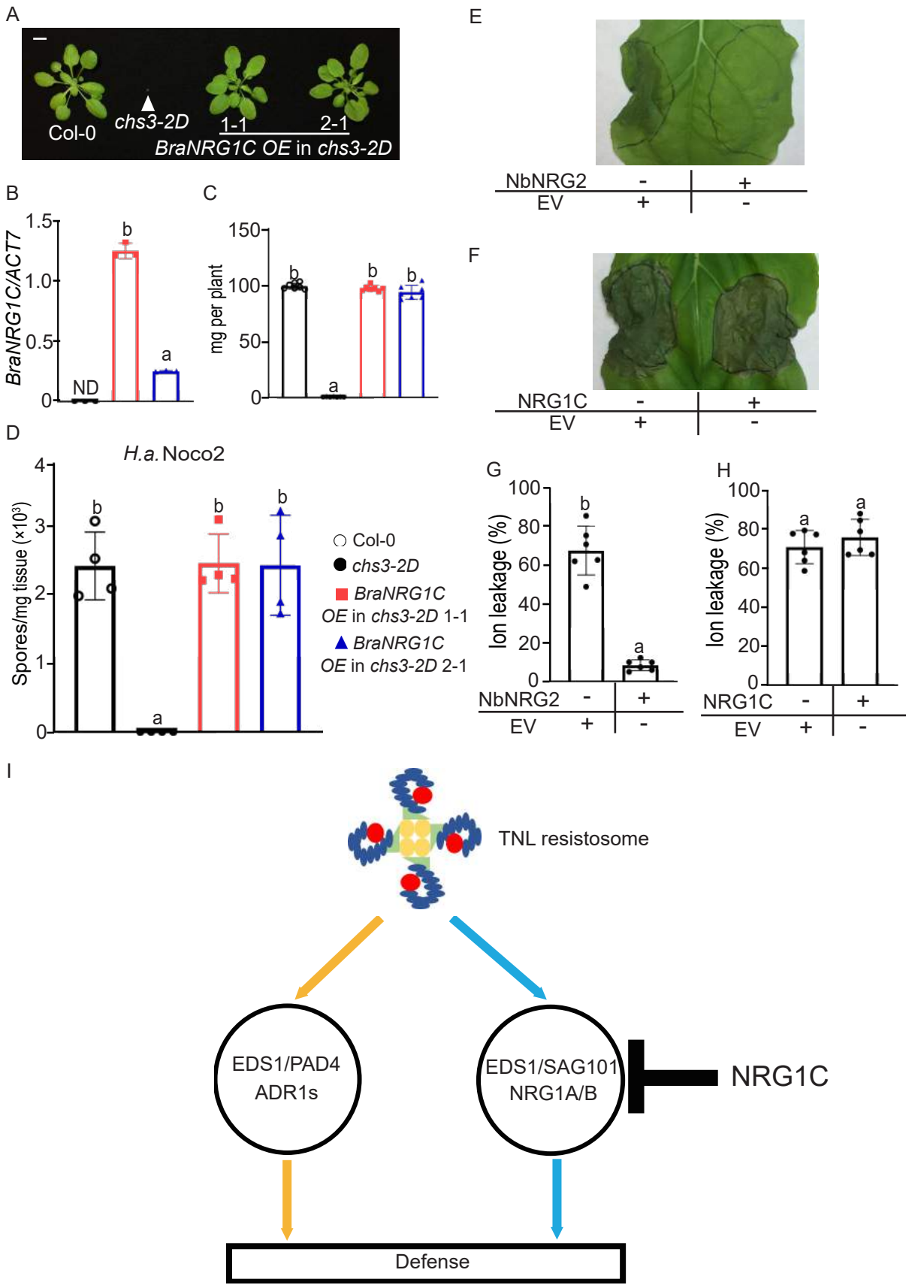

Figure 7. NRG1C-type N-terminally truncated hNLR from canola (*Brassica napus* L. cv. Westar) functions similarly as *A. thaliana* NRG1C.

A. Morphology of four-week-old soil-grown plants of Col-0, *chs3-2D*, and two independent transgenic lines of *BraNRG1C OE* into *chs3-2D* background. Bar = 1cm.

B. *BraNRG1C* gene expression in the indicated plants as determined by RT-PCR. Statistical significance is indicated by different letters ($p < 0.01$). Error bars represent means ± SE (n = 3). ND stands for Not Detectable. Two independent experiments were carried out with similar results. The color legends are included in D.

C. Fresh weights of plants in (A). Statistical significance is indicated by different letters ($p < 0.01$). Error bars represent means ± SE (n=7). The color legends are included in D.

D. Quantification of *H.a.* Noco2 sporulation in the indicated genotypes at 7 dpi with 10^5 spores per ml water. Statistical significance is indicated by different letters ($p < 0.01$). Error bars represent means ± SE (n=4). Three independent experiments were carried out with similar results.

E-F. HR observation of *N. benthamiana* leaves expressing the indicated proteins at 48 hpi following the infiltration of *P.s.t.* CUCPB5500 HopQ1-1 to deliver HopQ1-1 effector. Photographs were taken at 4 dpi after *P.s.t.* CUCPB5500 HopQ1-1 infiltration.

G-H. Ion leakage of *N. benthamiana* leaves upon *P.s.t.* CUCPB5500 HopQ1-1 infiltration under the same conditions as with E and F. Statistical significance is indicated by different letters ($p < 0.01$). Error bars represent means ± SE (n = 6). Three independent experiments were carried out with similar results.

I. A model of two defense modules downstream of TNL activation in Arabidopsis. An effector-induced TNL resistosome with NADase activity (Horsefield et al., 2019; Ma et al., 2020; Martin et al., 2020; Tian and Li, 2020; Wan et al., 2019) signals through two parallel modules, EDS1-PAD4-ADR1s and EDS1-SAG101-NRG1A/1B to activate defense responses. N-terminally truncated hNLR NRG1C antagonizes immunity mediated by its full-length neighbors NRG1A and NRG1B to avoid aberrant activation.

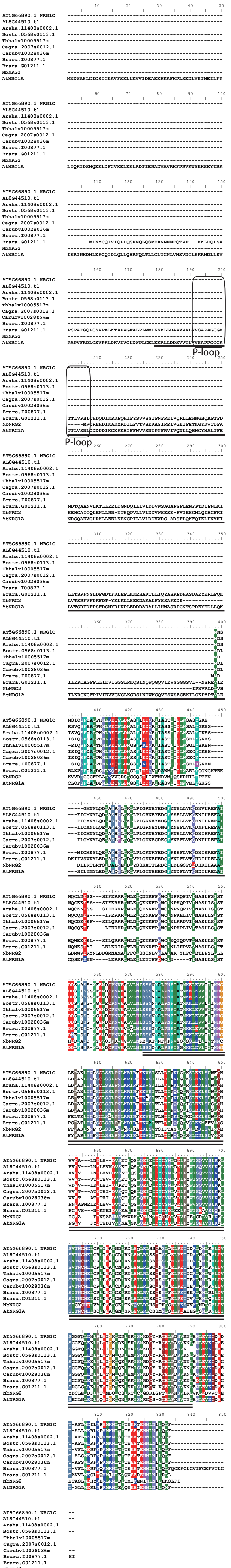

Figure S1. Full-length protein sequence alignment of NRG1C and its orthologs in different plant species.

Putative NRG1C orthologs were obtained from Phytozome (Brassicaceae species) and Sol Genomics Network (*N. benthamiana*) using *A. thaliana* NRG1C protein sequence as input. NB domain and LRR domain are indicated by single underline and double underline, respectively. P-loop motif is boxed in a black line.

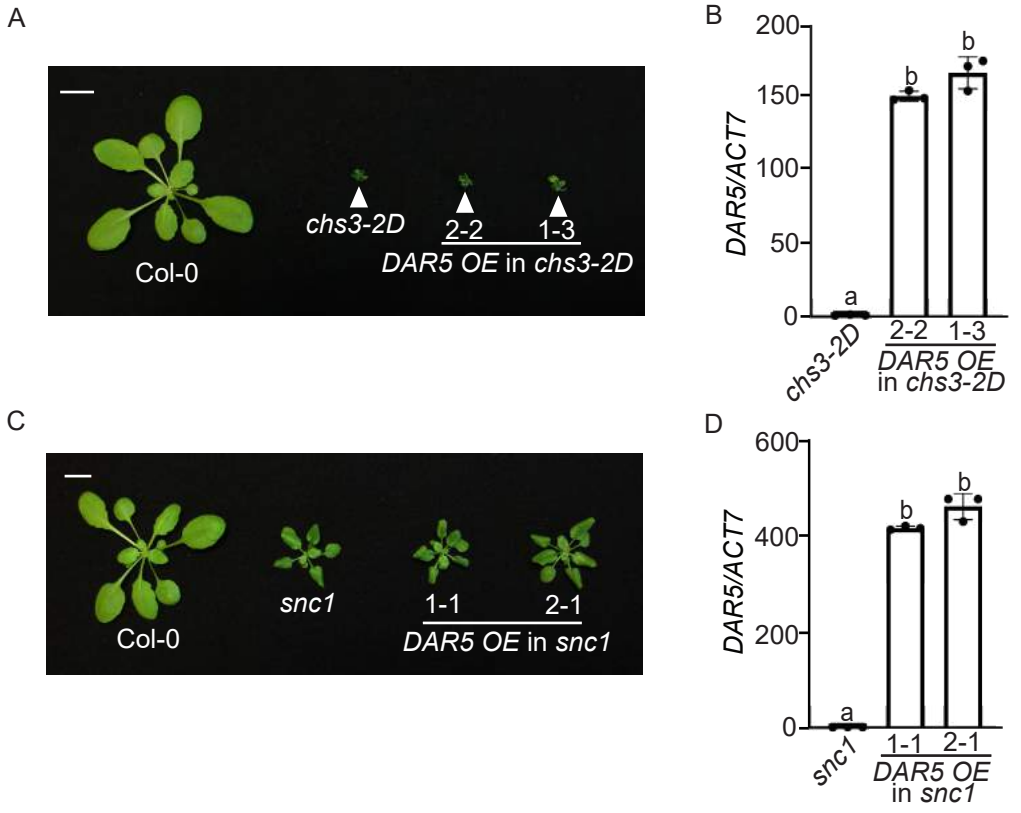

Figure S2. DAR5 has no effect on *chs3-2D* and *snc1*-mediated autoimmunity.

A. Morphology of four-week-old soil-grown plants of Col-0, *chs3-2D*, and two independent transgenic lines of *DAR5 OE* into *chs3-2D* background. *OE* stands for overexpression of *DAR5*. Bar = 1cm.

B. *DAR5* gene expression in the indicated plants as determined by RT-PCR (*chs3-2D* serves as control whose *DAR5* transcript level was set at 1.0). Statistical significance is indicated by different letters ($p < 0.01$). Error bars represent means ± SE (n = 3). Two independent experiments were carried out with similar results.

C. Morphology of four-week-old soil-grown plants of Col-0, *snc1*, and two independent transgenic lines of *DAR5 OE* into *snc1* background. *OE* stands for overexpression of *DAR5*. Bar = 1cm.

D. *DAR5* gene expression in the indicated plants as determined by RT-PCR (*snc1* serves as control whose *DAR5* transcript level was set at 1.0). Statistical significance is indicated by different letters ($p < 0.01$). Error bars represent means ± SE (n = 3). Two independent experiments were carried out with similar results.

Figure S3

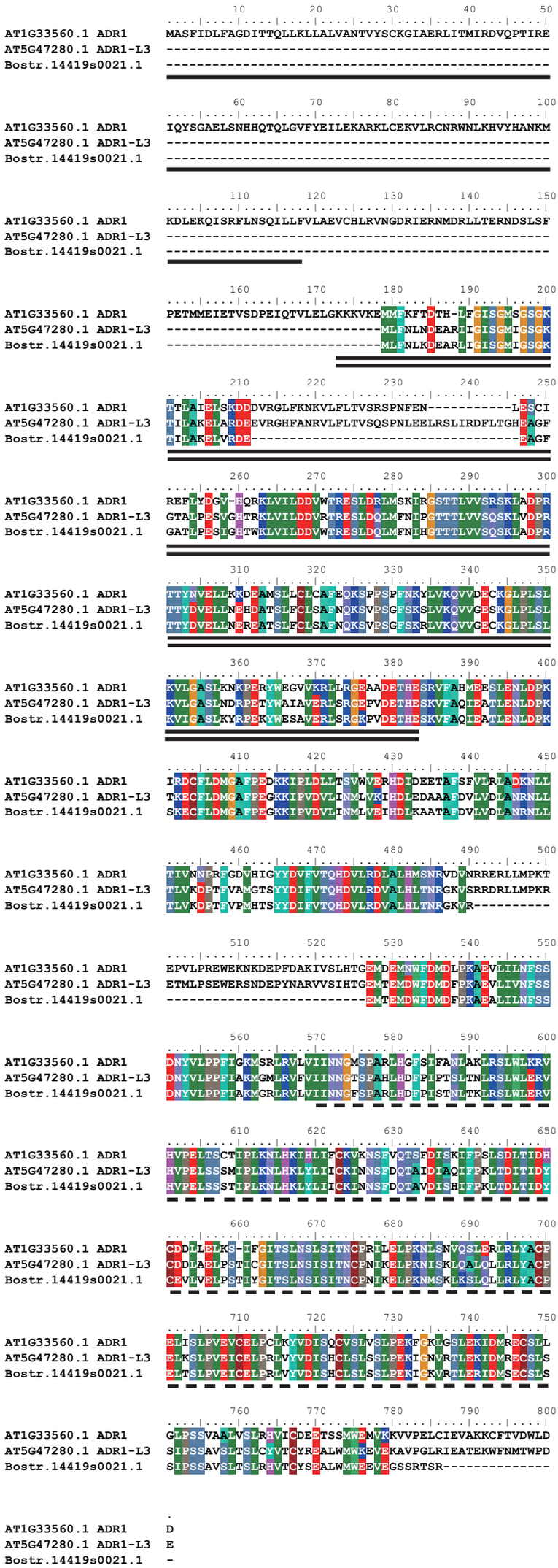

Figure S3. Full-length protein sequence alignment of ADR1-L3 and its orthologs in different plant species.

Putative ADR1-L3 orthologs were obtained from Phytozome using *A. thaliana* ADR1-L3 protein sequence as input. RPW8 domain, NB domain and LRR domain are indicated by single underline, double underline and dashed underline, respectively.

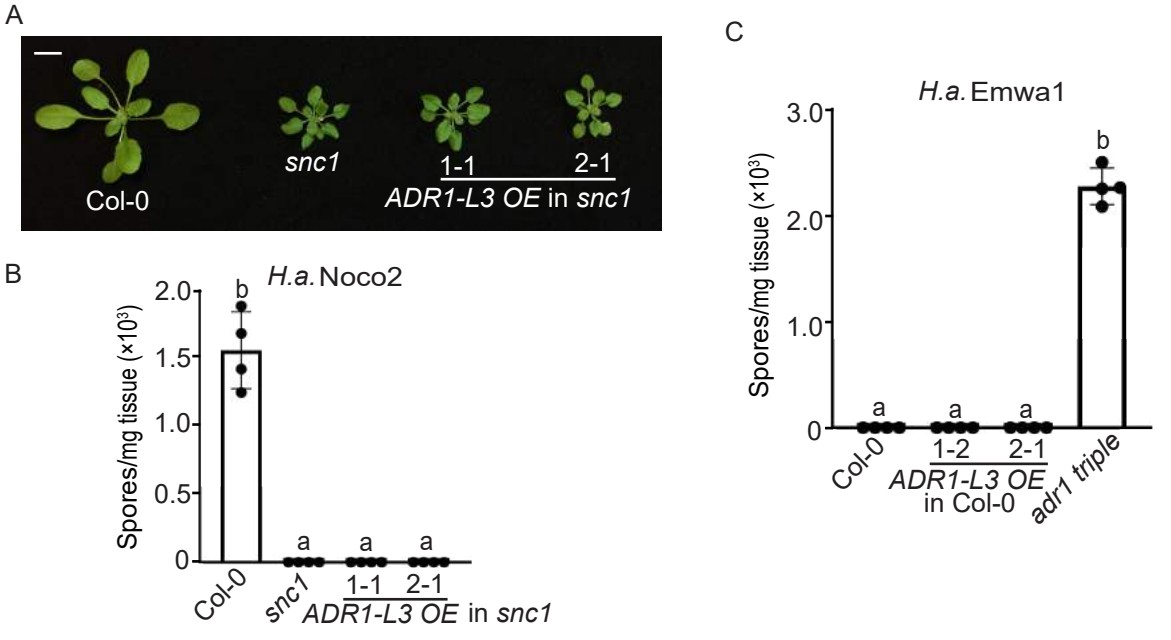

Figure S4. No immune-related phenotypes were observed in *ADR1-L3* overexpression lines.

A. Morphology of four-week-old soil-grown plants of Col-0, *snc1*, and two independent transgenic lines of *ADR1-L3 OE* into *snc1* background. *OE* stands for overexpression of *ADR1-L3*. Bar = 1cm.

B. Quantification of *H.a.* Noco2 sporulation in the indicated genotypes at 7 dpi with 10^5 spores per ml water. Statistical significance is indicated by different letters ($p < 0.01$). Error bars represent means ± SE (n=4). Three independent experiments were carried out with similar results.

C. Quantification of *H.a.* Emwa1 sporulation in the indicated genotypes at 7 dpi with 10^5 spores per ml water. Statistical significance is indicated by different letters ($p < 0.01$). Error bars represent means ± SE (n=4). Three independent experiments were carried out with similar results.

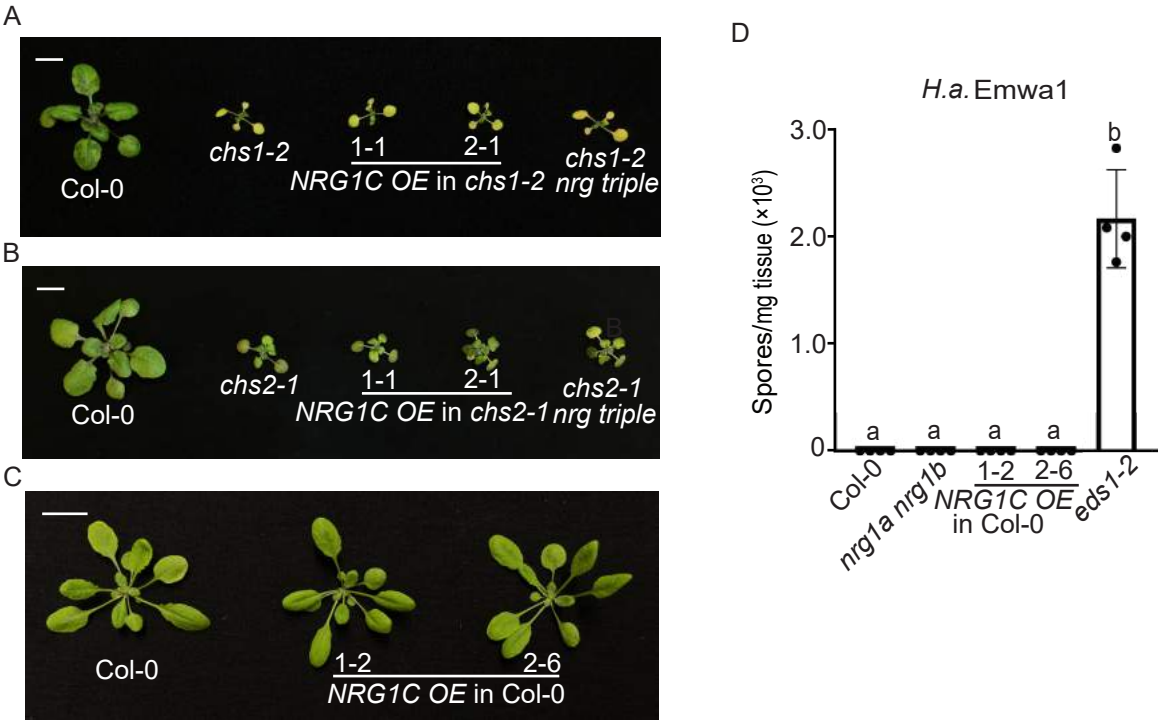

Figure S5. Overexpression of *NRG1C* has no effect on *chs1-2* or *chs2-1*-mediated autoimmunity.

A-B. Morphology of four-week-old soil-grown plants of Col-0, *chs1-2* (A), *chs2-1* (B) and two independent transgenic lines of *NRG1C OE* into *chs1-2* (A) and *chs2-1* (B) backgrounds. Plants were grown at 16 °C under long day conditions. Bar = 1cm.

C. Morphology of four-week-old soil-grown plants of Col-0 and two independent transgenic lines of *NRG1C OE* in Col-0 background. Bar = 1cm.

D. Quantification of *H.a.* Emwa1 sporulation in the indicated genotypes at 7 dpi with 10^5 spores per ml water. Statistical significance is indicated by different letters ($p < 0.01$). Error bars represent means ± SE (n=4). Three independent experiments were carried out with similar results.

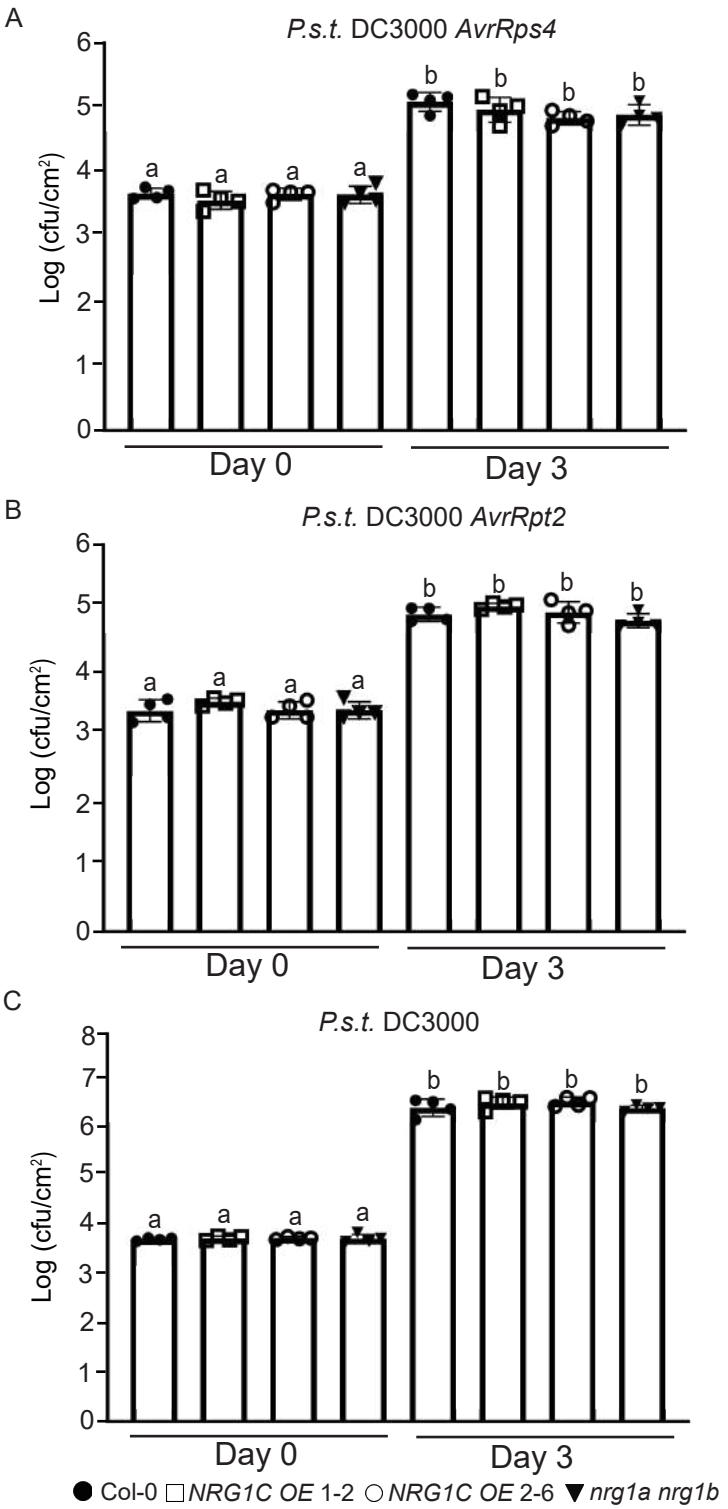

Figure S6. NRG1C does not affect TNL RPS4 or CNL RPS2-mediated bacterial growth and basal defense.

A-C. Growth of *P.s.t. avrRps4* (A), *avrRpt2* (B) and *P.s.t.* DC3000 (C) in four-week-old leaves of the indicated genotypes at 0 dpi and 3 dpi with bacterial inoculum of OD_{600} = 0.001. Statistical significance is indicated by different letters ($p < 0.01$). Error bars represent means ± SE (n=4). Three independent experiments were carried out with similar results.

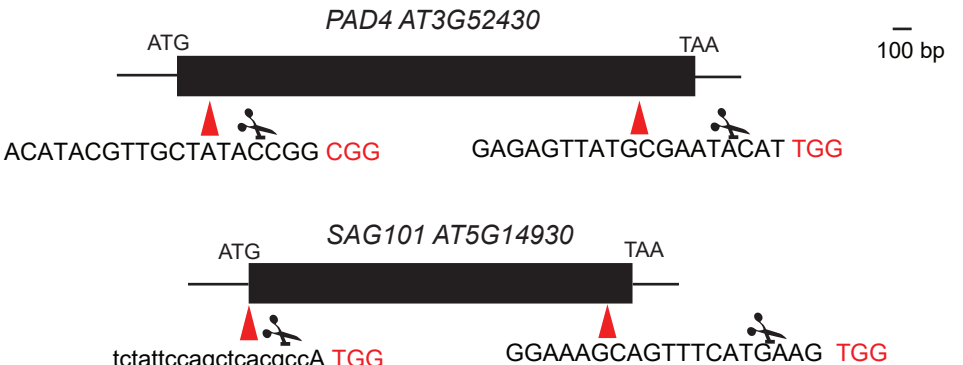

Figure S7. Schematic description of CRISPR/Cas9 construct design to delete *PAD4* or *SAG101*.

Red arrows indicate the location of two guide RNA target sites. Target sequences are shown in the below. The letters in red indicate the NGG PAM sequences. Scissors indicate where the Cas9 cut the genomic sequence.

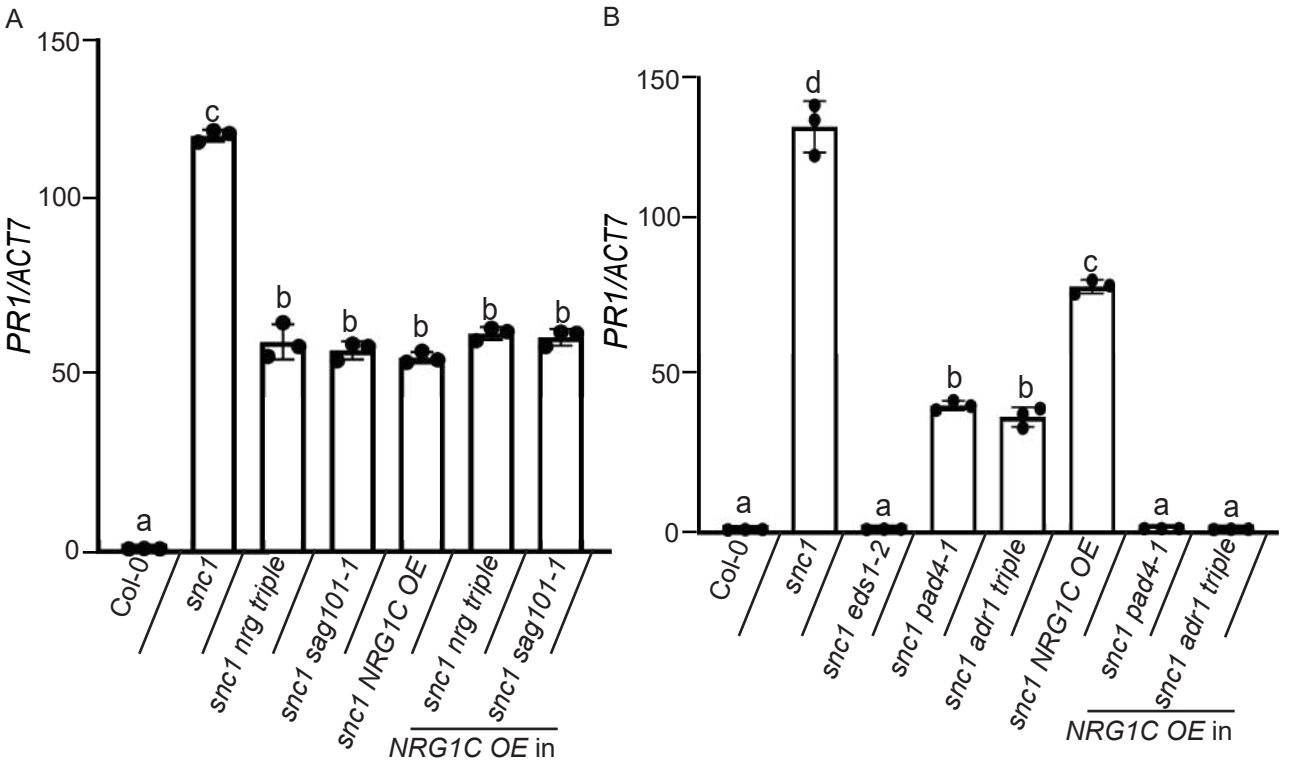

Figure S8. NRG1C works in the same pathway with the EDS1-NRG1-SAG101 module.

A-B. *PR1* gene expression in the indicated genotypes as determined by RT-PCR (Col-0 serves as control whose *PR1* transcript level was set at 1.0). Statistical significance is indicated by different letters ($p < 0.01$). Error bars represent means ± SE (n = 3). Two independent experiments were carried out with similar results.

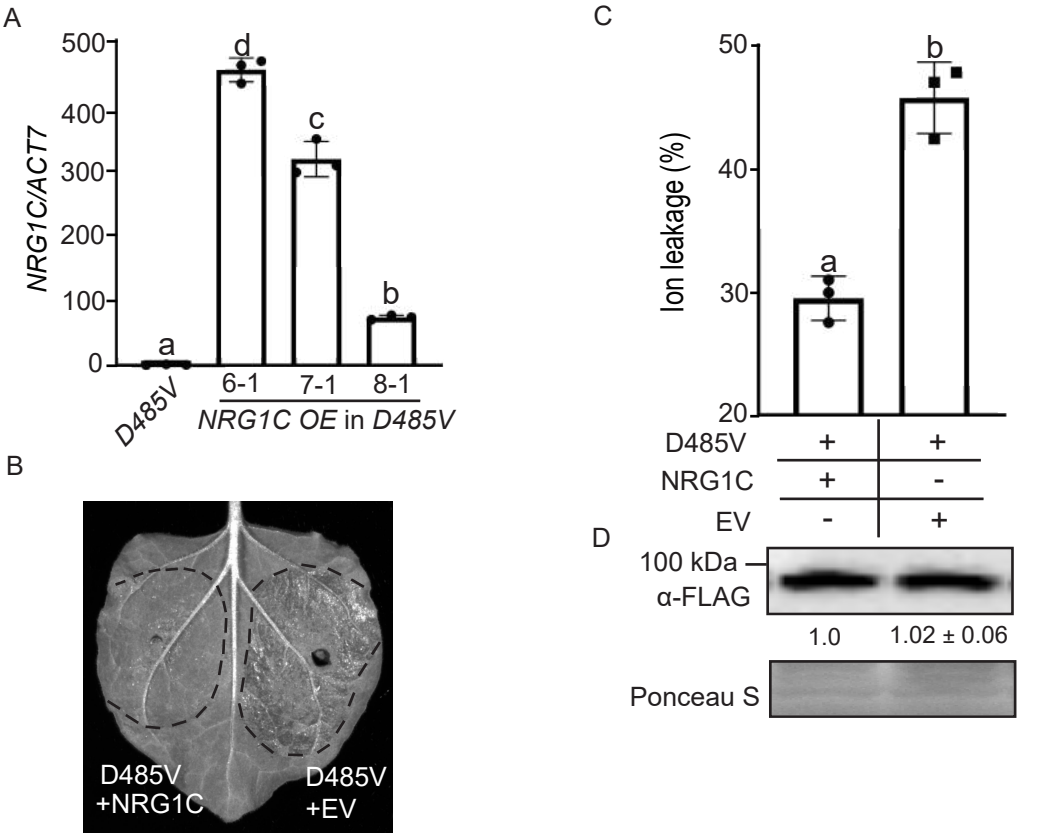

Figure S9. NRG1C antagonizes NRG1A D485V-mediated HR.

A. *NRG1C* gene expression in the indicated plants as determined by RT-PCR (*NRG1A D485V* serves as control whose *NRG1C* transcript level was set at 1.0). Statistical significance is indicated by different letters ($p < 0.01$). Error bars represent means ± SE (n = 3). Two independent experiments were carried out with similar results.

B. HR in the *N. benthamiana* leaves expressing NRG1A D485V-3FLAG and EV (Empty Vector) in the absence (right) or presence (left) of NRG1C. Photos were taken at 4 dpi. Three independent experiments were carried out with similar results.

C. Ion leakage of *N. benthamiana* leaves upon *Agrobacterium* infiltration under the same conditions as for B. Statistical significance is indicated by different letters ($p < 0.01$). Error bars represent means ± SE (n = 3). Three independent experiments were carried out with similar results.

D. Immunoblot analysis of protein levels of NRG1A D485V-3FLAG in leaves of B. Samples were harvest at 24 hpi, when no macroscopic HR was visible. Equal loading is shown by Ponceau S staining of a non-specific band. The numbers below represent the normalized ratio between the intensity of the protein band and the Ponceau S band ± SE (n=3). Molecular mass marker in kiloDaltons is indicated on the left.

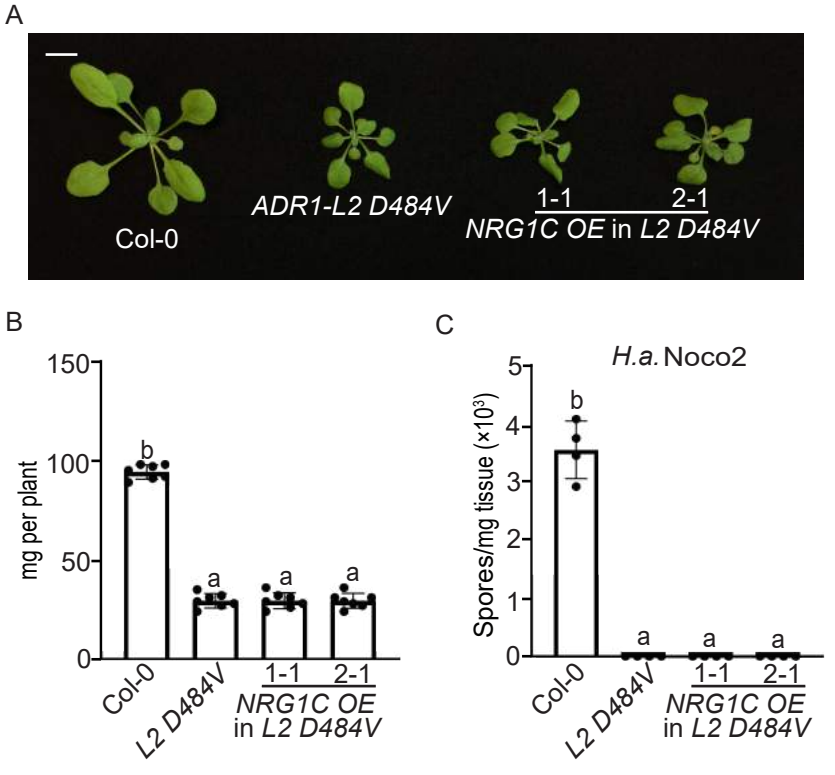

Figure S10. NRG1C does not influence the autoimmunity of *ADR1-L2 D484V*.

A. Morphology of three-week-old soil-grown plants of Col-0, *ADR1-L2 D484V*, and two independent transgenic lines of *NRG1C OE* into *ADR1-L2 D484V* background. *OE* stands for overexpression of *NRG1C*. Bar = 1cm.

B. Fresh weights of plants in (A). Statistical significance is indicated by different letters ($p < 0.01$). Error bars represent means ± SE (n=7).

C. Quantification of *H.a.* Noco2 sporulation in the indicated genotypes at 7 dpi with 10^5 spores per ml water. Statistical significance is indicated by different letters ($p < 0.01$). Error bars represent means ± SE (n=4). Three independent experiments were carried out with similar results.

Figure S11

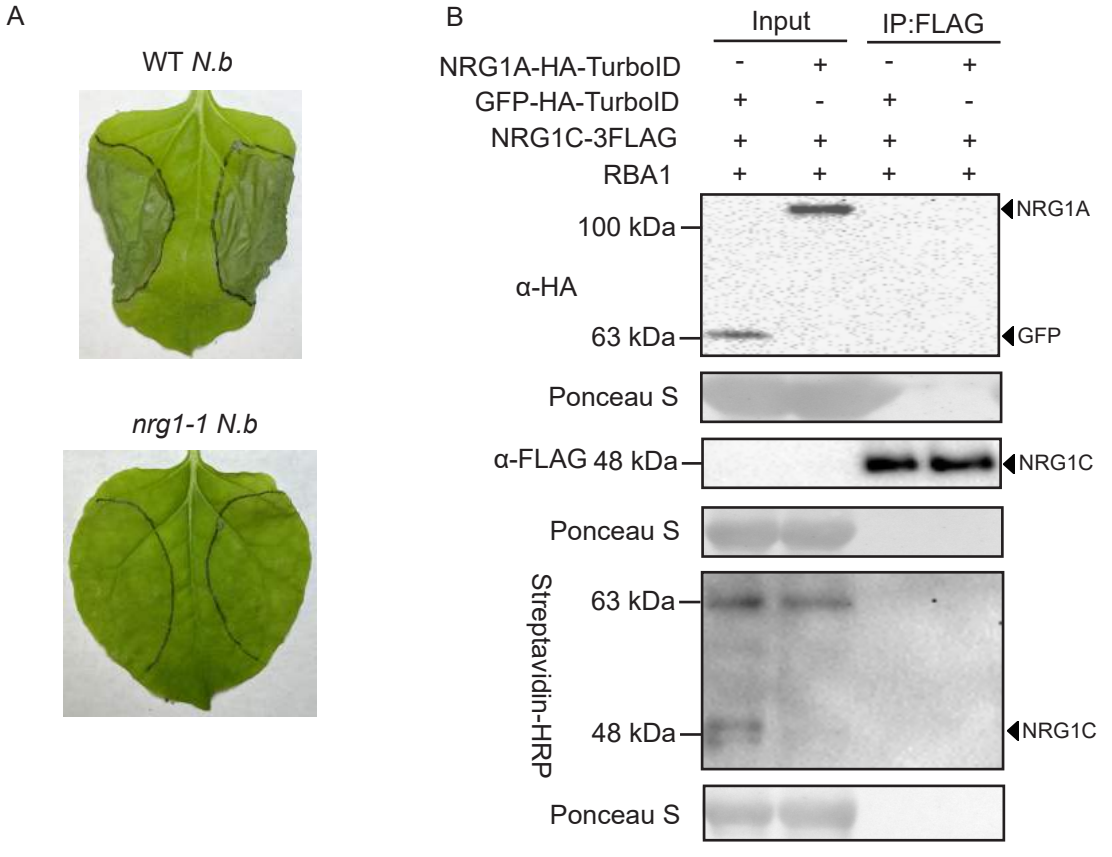

Figure S11. NRG1C does not associate with full-length NRG1A.

A. HR in the WT or *nrg1-1 N. benthamiana* leaves expressing RBA1. Photos were taken at 2 dpi. Three independent experiments were carried out with similar results.

B. Immunoprecipitation of NRG1C-3FLAG and biotinylation of NRG1C-3FLAG by NRG1A-HATurboID in *N. benthamiana* in the presence of RBA1. Immunoprecipitation was carried out with anti-FLAG beads. The 3FLAG-tagged proteins were detected using an anti-FLAG antibody. The HA-TurboID-tagged proteins were detected using an anti-HA antibody. The biotinylated proteins were detected using Streptavidin-HRP. Molecular mass marker in kiloDaltons is indicated on the left. Three independent experiments were carried out with similar results.

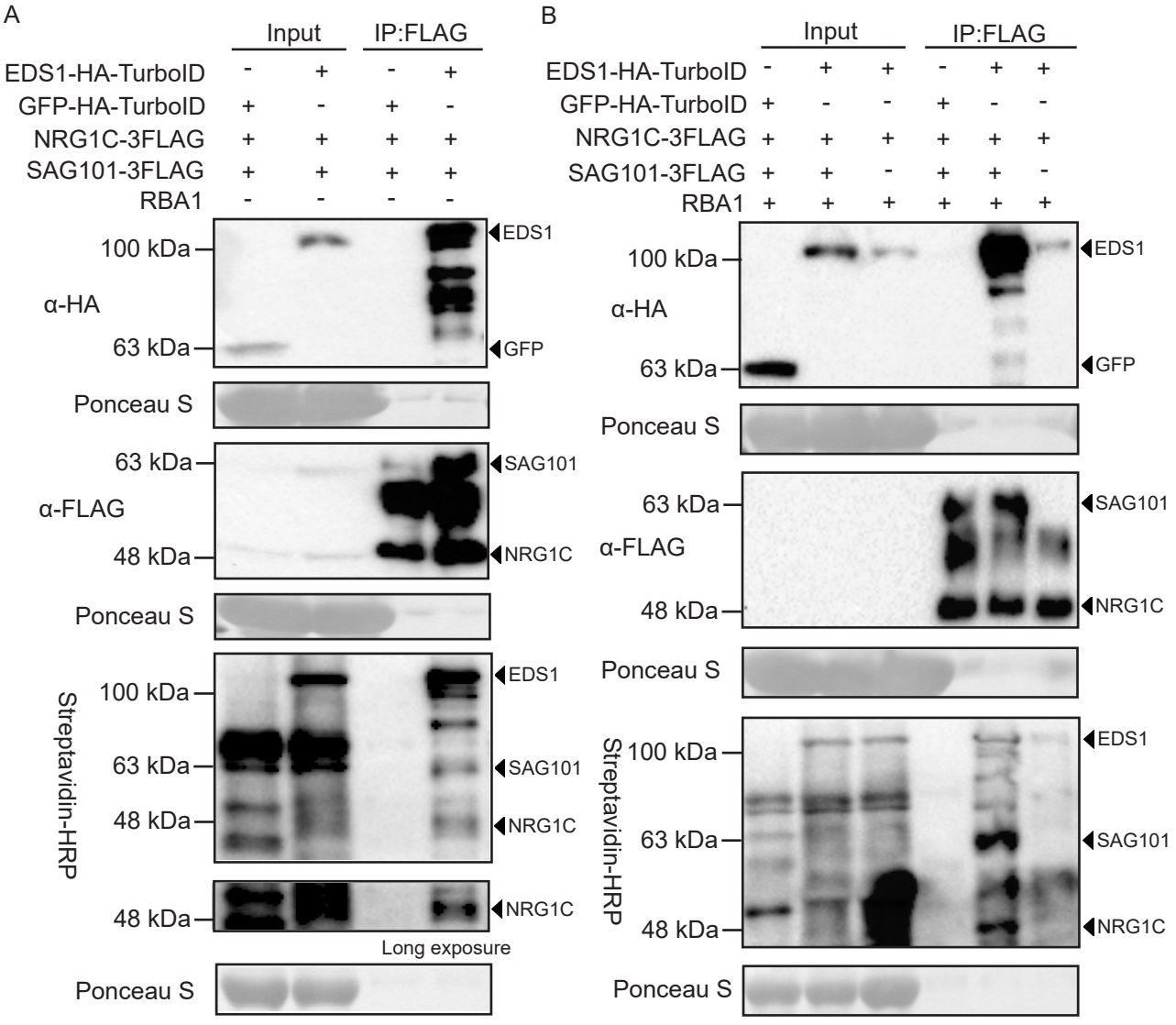

Figure S12. The association between NRG1C with EDS1-SAG101 complex depends on TIR induction and SAG101.

A. Immunoprecipitation and biotinylation of NRG1C-3FLAG and SAG101-3FLAG by EDS1-HA-TurboID in *N. benthamiana* in the absence of RBA1. Immunoprecipitation was carried out with anti-FLAG beads. The 3FLAG-tagged proteins were detected using an anti-FLAG antibody. The HA-TurboID-tagged proteins were detected using an anti-HA antibody. The biotinylated proteins were detected using Streptavidin-HRP. Molecular mass marker in kiloDaltons is indicated on the left. Three independent experiments were carried out with similar results.

B. Immunoprecipitation and biotinylation of NRG1C-3FLAG or/and SAG101-3FLAG by EDS1-HA-TurboID in *N. benthamiana*. Immunoprecipitation was carried out with anti-FLAG beads. The 3FLAG-tagged proteins were detected using an anti-FLAG antibody. The HA-TurboID-tagged proteins were detected using an anti-HA antibody. The biotinylated proteins were detected using Streptavidin-HRP. Molecular mass marker in kiloDaltons is indicated on the left. Three independent experiments were carried out with similar results.

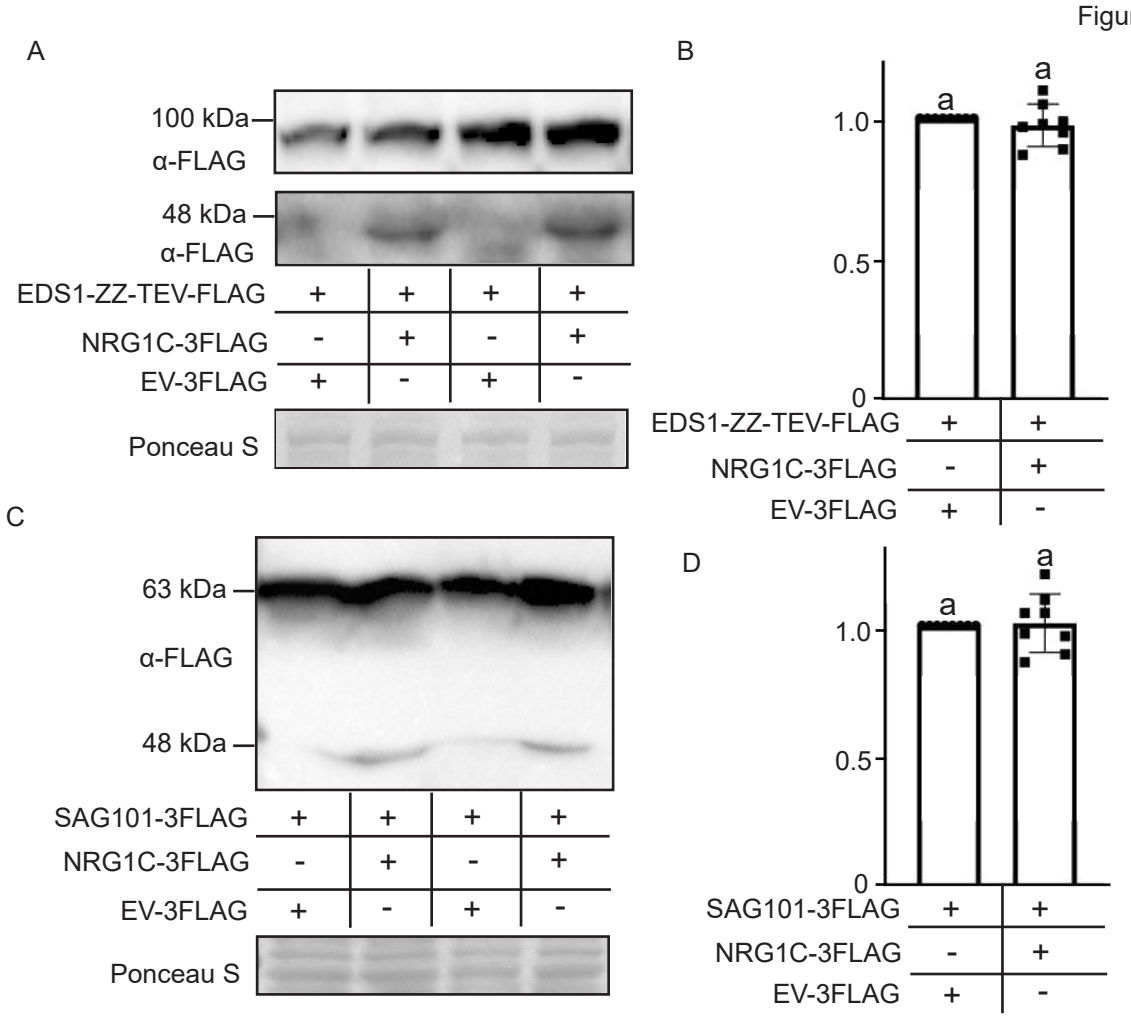

Figure S13. Overexpression of *NRG1C* does not affect the protein levels of EDS1 and SAG101.

A. Immunoblot analysis of protein levels of EDS1-ZZ-TEV-FLAG in the absence or presence of NRG1C-3FLAG. Equal loading is shown by Ponceau S staining of a non-specific band. Molecular mass marker in kiloDaltons is indicated on the left.

B. Quantification of band intensity of (A). The numbers represent the normalized ratio between the intensity of the protein band and the Ponceau S band ± SE (n=8).

C. Immunoblot analysis of protein levels of SAG101-3FLAG in the absence or presence of NRG1C-3FLAG. Equal loading is shown by Ponceau S staining of a non-specific band. Molecular mass marker in kiloDaltons is indicated on the left.

D. Quantification of band intensity of C. The numbers represent the normalized ratio between the intensity of the protein band and the Ponceau S band ± SE (n=8).

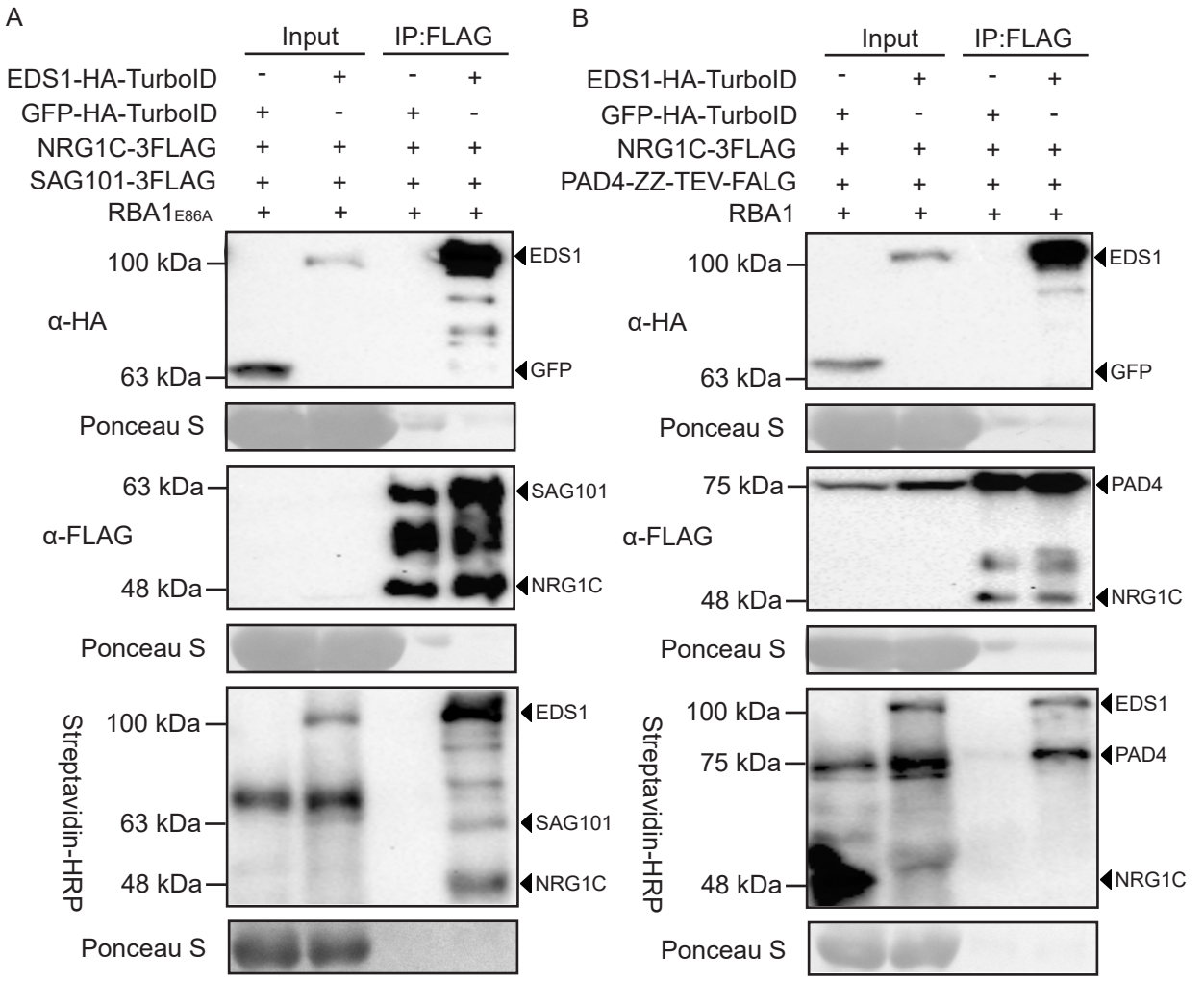

C

Treatment	-RBA1	+RBA1	+RBA1$_{E86A}$
Intensity	1.01	3.58	1.51

Figure S14. TIR NADase enzyme activity promotes the association between NRG1C with EDS1-SAG101 complex, and NRG1C does not associate with the EDS1-PAD4 complex.

A. Immunoprecipitation and biotinylation of NRG1C-3FLAG and SAG101-3FLAG by EDS1-HA-TurboID in *N. benthamiana* in the presence of RBA1$_{E86A}$. Immunoprecipitation was carried out with anti-FLAG beads. The 3FLAG-tagged proteins were detected using an anti-FLAG antibody. The HA-TurboID-tagged proteins were detected using an anti-HA antibody. The biotinylated proteins were detected using Streptavidin-HRP. Molecular mass marker in kiloDaltons is indicated on the left. Three independent experiments were carried out with similar results.

B. Immunoprecipitation and biotinylation of NRG1C-3FLAG and PAD4-ZZ-TEV-FLAG by EDS1-HA-TurboID in *N. benthamiana* in the presence of RBA1. Immunoprecipitation was carried out with anti-FLAG beads. The ZZ-TEV-FLAG and 3FLAG-tagged proteins were detected using an anti-FLAG antibody. The HA-TurboID-tagged proteins were detected using an anti-HA antibody. The biotinylated proteins were detected using Streptavidin-HRP. Molecular mass marker in kiloDaltons is indicated on the left. Three independent experiments were carried out with similar results.

C. The normalized ratio between the intensity of the NRG1C band and the SAG101 band in different treatments. As EDS1 constitutively associates with SAG101, SAG101 bands were used as controls.

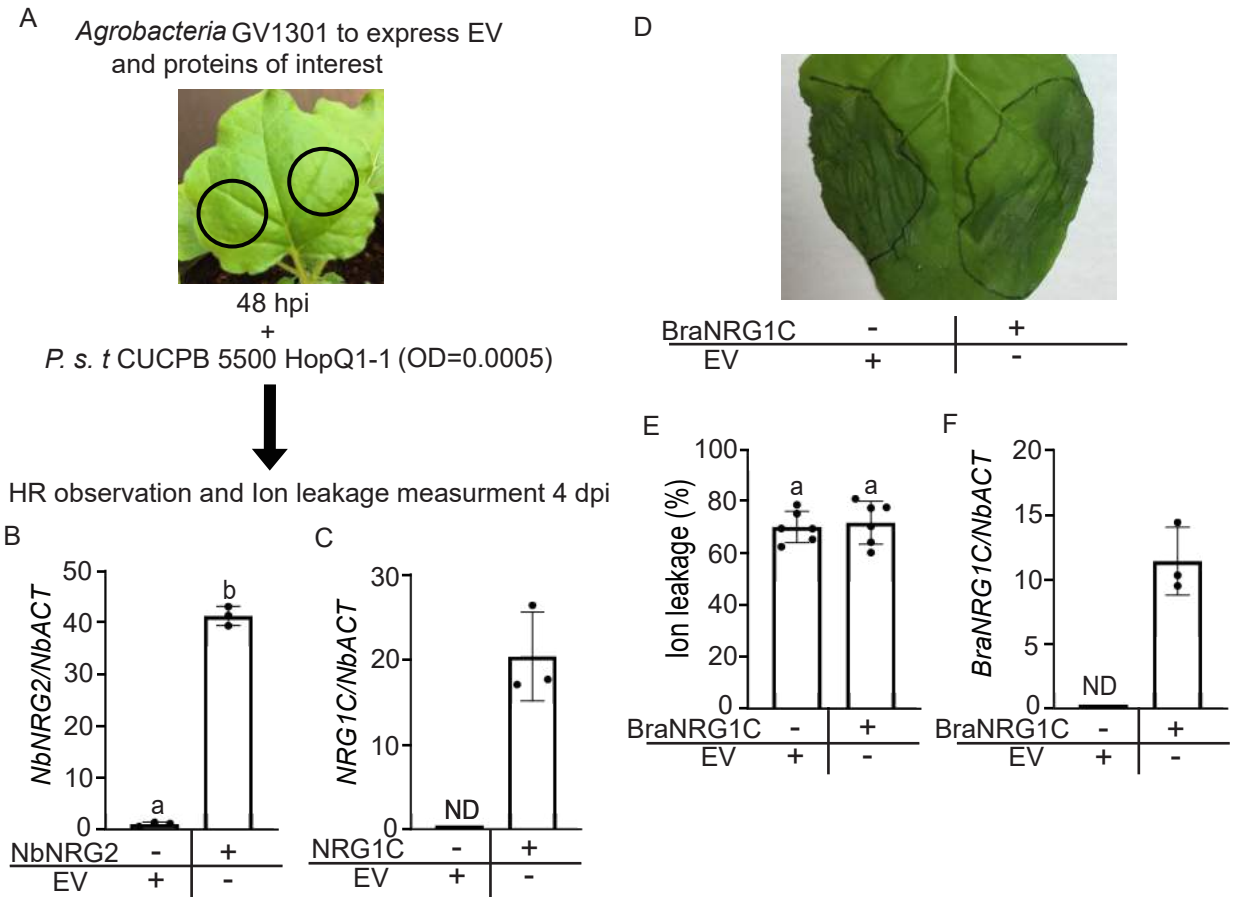

Figure S15. Brassicaceae NRG1C ortholog does not influence HopQ1-1-mediated HR in *N. benthamiana*.

A. Schematic showing *N. benthamiana* transient expression assays to test protein functionalities in HopQ1-1-dependent HR by infiltrating with *P.s.t.* CUCPB5500 HopQ1-1 (see Methods for details).

B-C. *NbNRG2* (B) and *NRG1C* (C) genes expression in the indicated leaves as determined by RT-PCR. Statistical significance is indicated by different letters ($p < 0.01$). Error bars represent means ± SE (n = 3). The *NbNRG2* transcript level in the presence of EV treatment was set at 1.0. Two independent experiments were carried out with similar results.

D. HR in the *N. benthamiana* leaves expressing the indicated proteins at 48 hpi following the infiltration of *P.s.t.* CUCPB5500 HopQ1-1 to deliver HopQ1-1 effector. Photographs were taken at 4 dpi after *P.s.t.* CUCPB5500 HopQ1-1 infiltration.

E. Ion leakage of *N. benthamiana* leaves upon *P.s.t.* CUCPB5500 HopQ1-1 infiltration in the same conditions as for the photographs in D. Statistical significance is indicated by different letters ($p < 0.01$). Error bars represent means ± SE (n = 6). Three independent experiments were carried out with similar results.

F. *BraNRG1C* gene expression in the indicated leaves as determined by RT-PCR. Error bars represent means ± SE (n = 3). Two independent experiments were carried out with similar results.

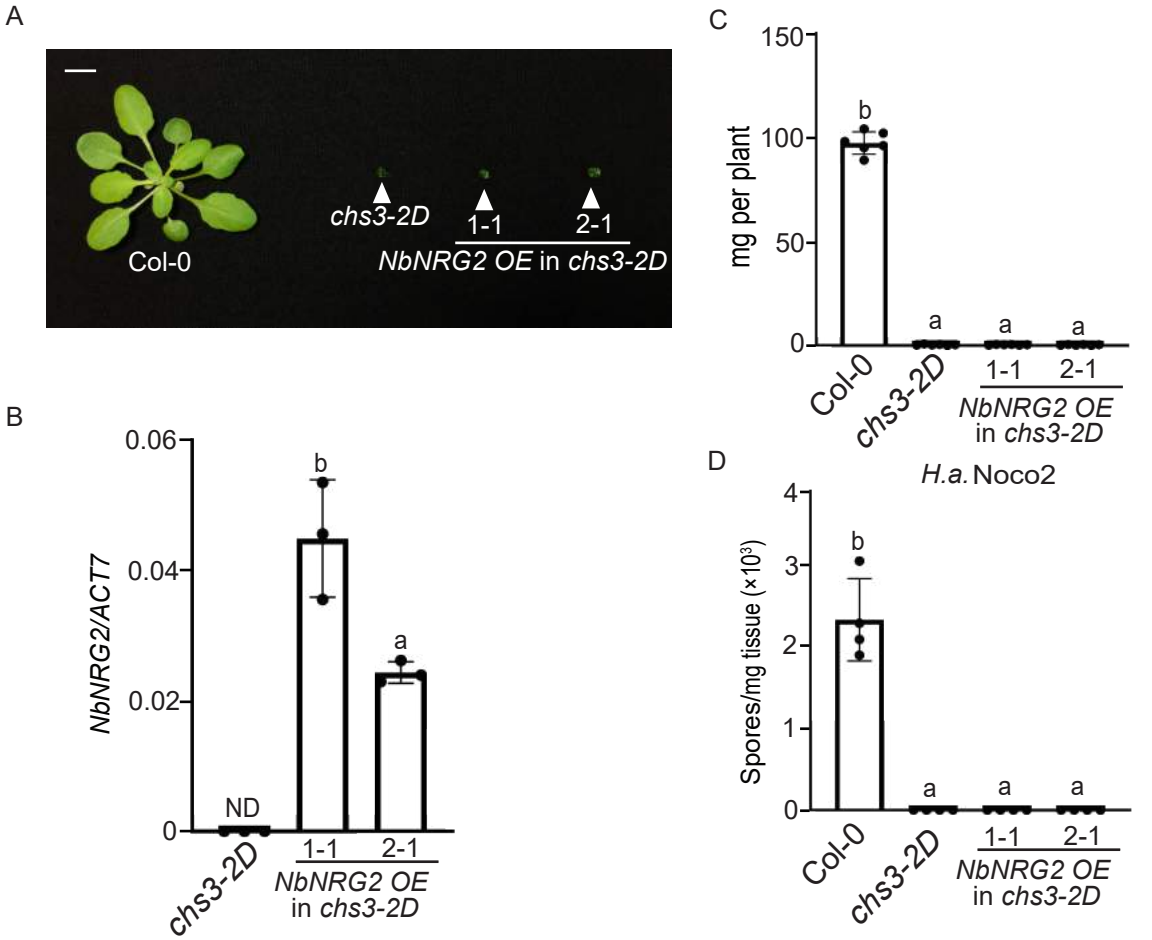

Figure S16. NbNRG2 does not influence *chs3-2D*-mediated autoimmunity.

A. Morphology of four-week-old soil-grown plants of Col-0, *chs3-2D*, and two independent transgenic lines of *NbNRG2 OE* into *chs3-2D* background. *OE* stands for overexpression of *NbNRG2*. Bar = 1cm.

B. *NbNRG2* expression level in the indicated plants as determined by RT-PCR. Statistical significance is indicated by different letters ($p < 0.05$). Error bars represent means ± SE (n = 3). Three independent experiments were carried out with similar results.

C. Fresh weights of plants in (A). Statistical significance is indicated by different letters ($p < 0.01$). Error bars represent means ± SE (n=6).

D. Quantification of *H.a.* Noco2 sporulation in the indicated genotypes at 7 dpi with 10^5 spores per ml water. Statistical significance is indicated by different letters ($p < 0.01$). Error bars represent means ± SE (n=4). Three independent experiments were carried out with similar results.

Table S1. The genome arrangement of NRG1C in plant species.

Species	*NRG1C* gene arrangement
Arabidopsis thaliana	
Arabidopsis lyrata	
Arabidopsis halleri	
Boechera stricta	
Capsella grandiflora	
Capsella rubella	
Eutrema salsugineum	
Brassica rapa	

Arrows in tandem indicate tandemly arranged genes, while arrows in rows indicate randomly assorted genes on different scaffolds. All sequences were obtained from Phytozome. *A. thaliana* (*AT5G66910*, *AT5G66900*, *AT5G66890*); *Arabidopsis lyrate* (*AL8G44490*, *AL8G44500*, *AL8G44510*); *Arabidopsis haller* (*Araha.11408s0003.1*, *Araha.11408s0002.1*); *Boechera stricta* (*Bostr.27102s0001.1*; *Bostr.0568s0113.1*); *Capsella grandiflora* (*Cagra.2007s0011.1*, *Cagra.2007s0012.1*); *Capsella rubella* (*Carubv 10027991m*, *Carubv10028036m*); *Eutrema salsugineum* (*Thhalv10003662m*, *Thhalv10005443m*, *Thhalv10005517m*; *Thhalv10020099m*); *Brassica rapa* (*Brara.I00877.1*, *Brara.I00876.1*; *Brara.G01212.1*, *Brara.G01211.1*; *Brara.B03562.1*; *Brara.F02778.1*). All truncated NRG1C orthologs are labeled with yellow arrows. Orange arrow indicates *Brara.*G01211.1.

Table S2. The genome arrangement of *NL* truncated genes in *Arabidopsis*.

NLs Cluster	Genes arrangement
1	4G19060 4G19050
2	5G45440 .... 5G45490 .... 5G45510 5G45520
3	1G61310 1G61300
4	5G38340 5G38344 5G38350
5	4G09360 .... 4G09420 4G09430

Arrows in tandem indicate tandemly arranged genes. Dashed line indicates two genes are clustered, but not tandemly arranged. Gene codes are shown under the arrows. Orange, yellow, black, and blue arrows indicate CN, NL, full-length NLR, TIR-only proteins, respectively.

Table S3. The list of primers used in this study.

Name	Sequence	Purpose
NRG1C-KpnI-F	gcgcggtaccATG AATTCGAATTCGATTCA	To generate pCambia 1305 NRG1C
NRG1C-SpeI-R	gactagtTTAAAACAGTTGAAGCAAGTTGA	
NRG1C-KpnI-F	gcgcggtaccATG AATTCGAATTCGATTCA	To generate pCambia 1300 NRG1C-3FLAG
NRG1C-SpeI(ns)-R	gactagtAAACAGTTGAAGCAAGTTGAG	
1C-Y71ST-F	atagGAGAAATGAGTAGGAAGATGGTTTCTAC	To generate pCambia 1305 NRG1C T71STOP
1C-Y71ST-R	GTAGAAACCATCTTCCTACTCATTTCTCCTAT	
DAR5-SfiI-F	CCCGGCCGTCAAGGCCATGCCGATCTCGGATGT	To generate pHan DAR5
DAR5-SfiI-R	GCCGGCCCATGAGGCCTTACCTCCGGCGAAGAAT	
SAG101-CK-F	gagtaacaaattcgtcttggag	To genotype SAG101 CRISPR allele
SAG101-CK-R	CTAAGAGTTGTTGCGATTGATG	
SAG101-homo-R	GAATGATGGGTTGTTCTCG	
PAD4-checking-F	ccgattacataggatcacatgc	To genotype PAD4 CRISPR allele
PAD4-checking-R	CACCATCACACTACATGTTGG	
PAD4-homo-F	CAGATACGCGAGCACAAC	
NRG1C-RT-F	CTTCCTATTGGGAGAAATGAG	NRG1C RT primers
NRG1C-RT-R	CACAACCTTCAATTCCTTC	
DAR5-RT-F	CTCCTCTTAGCATGTGTGGT	DAR5 RT primers
DAR5-RT-R	CCATCAGCTTCATGAACAGG	
NRG1-KpnI-F	gcgcggtaccCATGAACGATTGGGCTAGTTTG	To generate pBNRG1AHATurboID
NRG1-SpeI(NS)-R	gactagtcAAACATTTGAAGCAAGTTCAGGT	
SAG101-KpnI-F	gcgcggtaccATGGAGTCTTCTTCTTCACT	

SAG101-BamHI(NS)-R	cgcggatccTTGTGACTTACCATAACTCTCG	To generate pCambia SAG101-3FLAG
Bra877-DraIII-F	cggcggCACTCAGTGATGATGGATTCGATCCAAAG	To generate pBBraNRG1C
Bra877-DraIII-R	cggcggCACATGGTGTCATATACTTCCTAATGTTACAAA	
Bra877-RT-F	TGCCTCCCACAATCTTC	BraNRG1C RT primers
Bra877-RT-R	GCAAATTCTCTCGAGATGTTG	
NRG2-KpnI-F	gcgcggtaccatggtttgtcgagagcatga	To generate pBNbNRG2
NRG2-SpeI-R	GGACTAGTTCAGATAAATAACGATTTATGCAGC	
NRG2-RT-F	tgtgcgacttgatcttgttc	NbNRG2 RT primers
NRG2-RT-R	GCAGCAGCACATCACTCT	
PAD4_BsF	ATATATGGTCTCGATTGACATACGTTGCTATACCGGGTT	To generate PAD4 CRISPR
PAD4_F0	TGACATACGTTGCTATACCGGGTTTTAGAGCTAGAAATAGC	
PAD4_R0	AACATGTATTCGCATAACTCTCCAATCTCTTAGTCGACTCTAC	
PAD4_BsR	ATTATTGGTCTCGAAACATGTATTCGCATAACTCTCC	
SAG101_BsF	ATATATGGTCTCGATTGtctattccagctcacgccAGTT	To generate SAG101 CRISPR
SAG101_F0	TGtctattccagctcacgccAGTTTTAGAGCTAGAAATAGC	
SAG101_R0	AACCTTCATGAAACTGCTTTCCCAATCTCTTAGTCGACTCTAC	
SAG101_BsR	ATTATTGGTCTCGAAACCTTCATGAAACTGCTTTCCC	